Optimizing CMB Polarization Experiments to Constrain Inflationary Physics

Raul Jimenez

ICREA & University of Barcelona

Icc.ub.edu/~jimenez

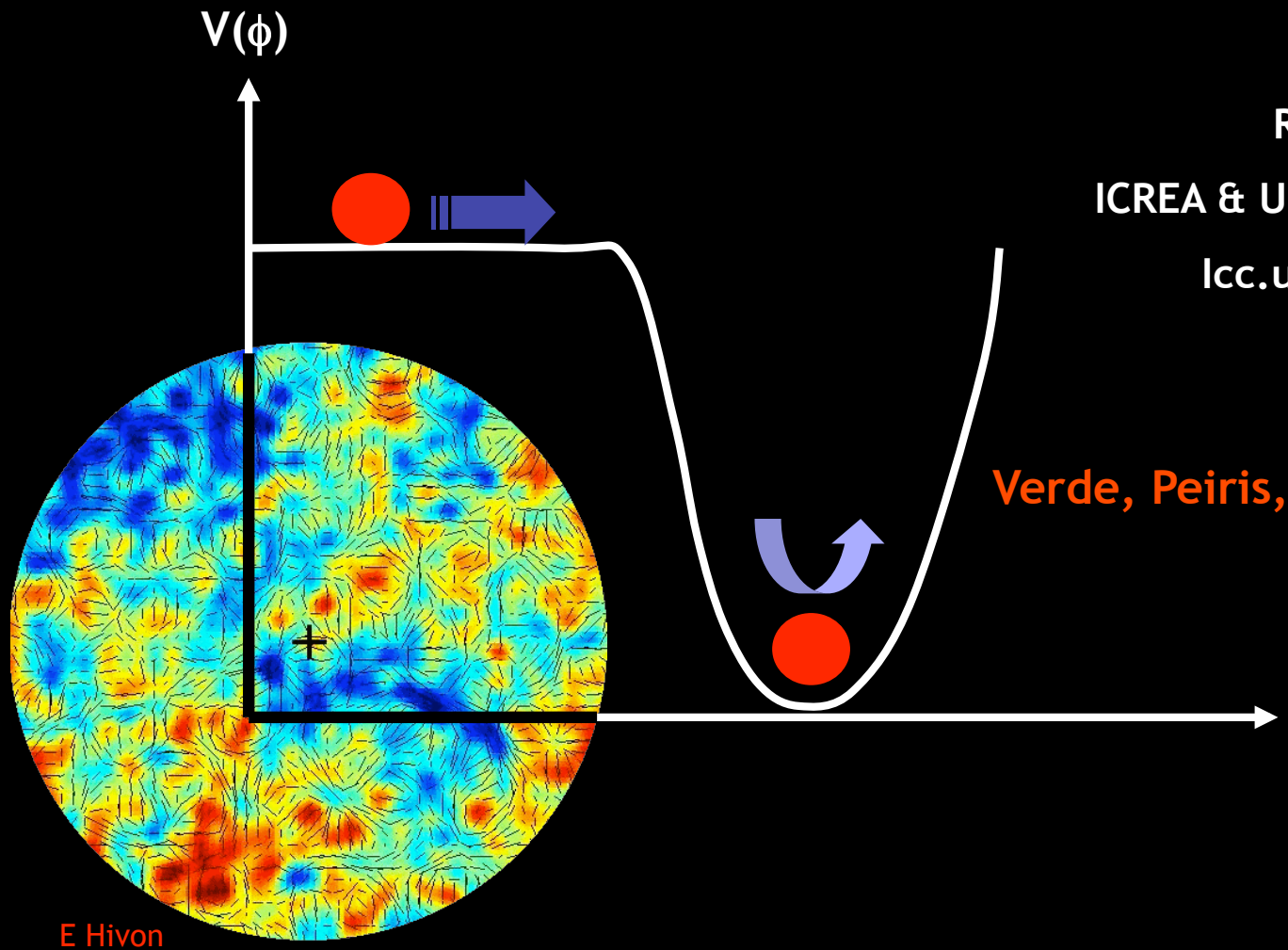

Verde, Peiris, Jimenez JCAP (2006)

Inflation

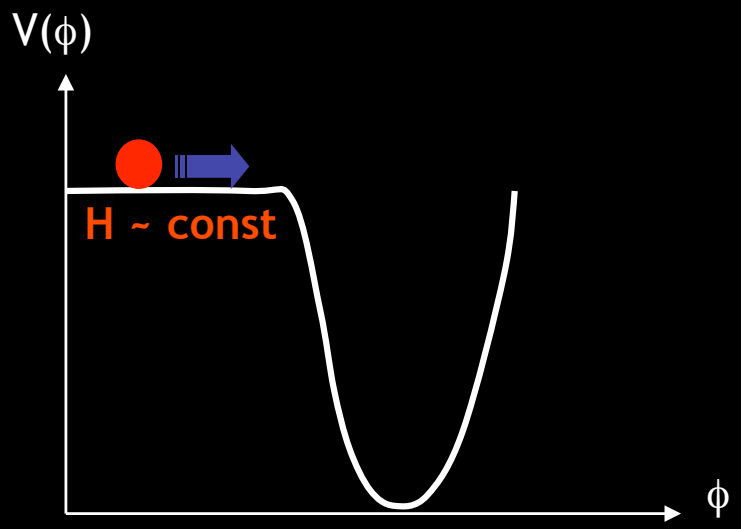

Solves cosmological problems (Horizon, flatness).

Cosmological perturbations arise from quantum fluctuations, evolve classically.

Guth (1981), Linde (1982), Albrecht & Steinhardt (1982), Sato (1981), Mukhanov & Chibisov (1981), Hawking (1982), Guth & Pi (1982), Starobinsky (1982), J. Bardeen, P.J. Steinhardt, M. Turner (1983), Mukhanov et al. 1992), Parker (1969), Birrell and Davies (1982)

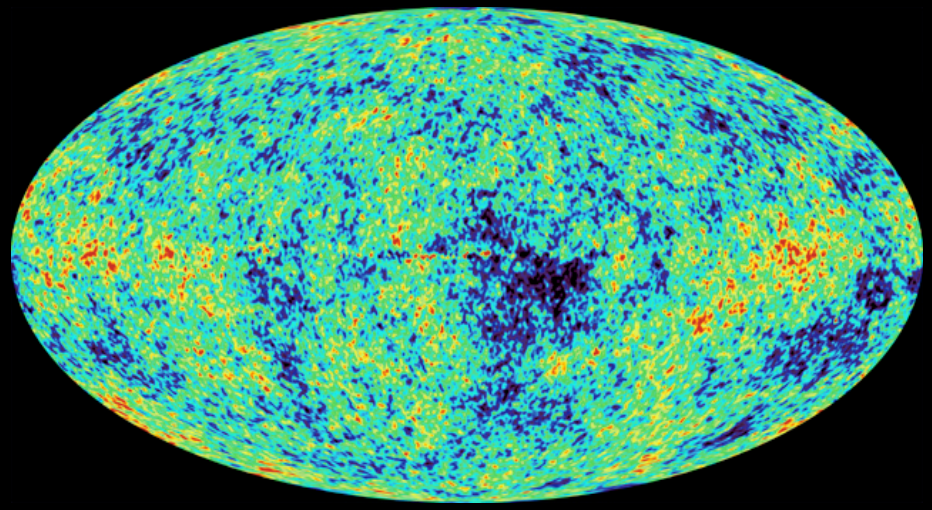

Horizon problem

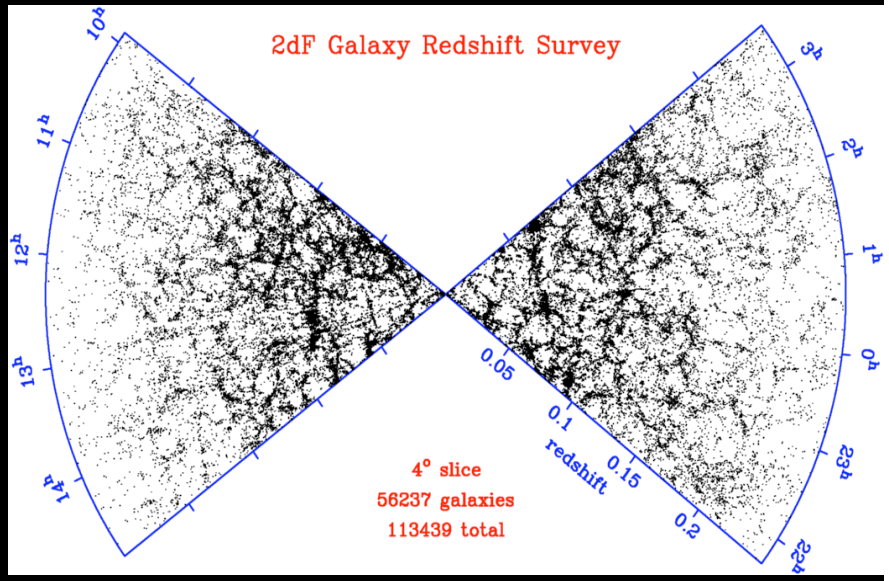

Structure Problem

Flatness problem

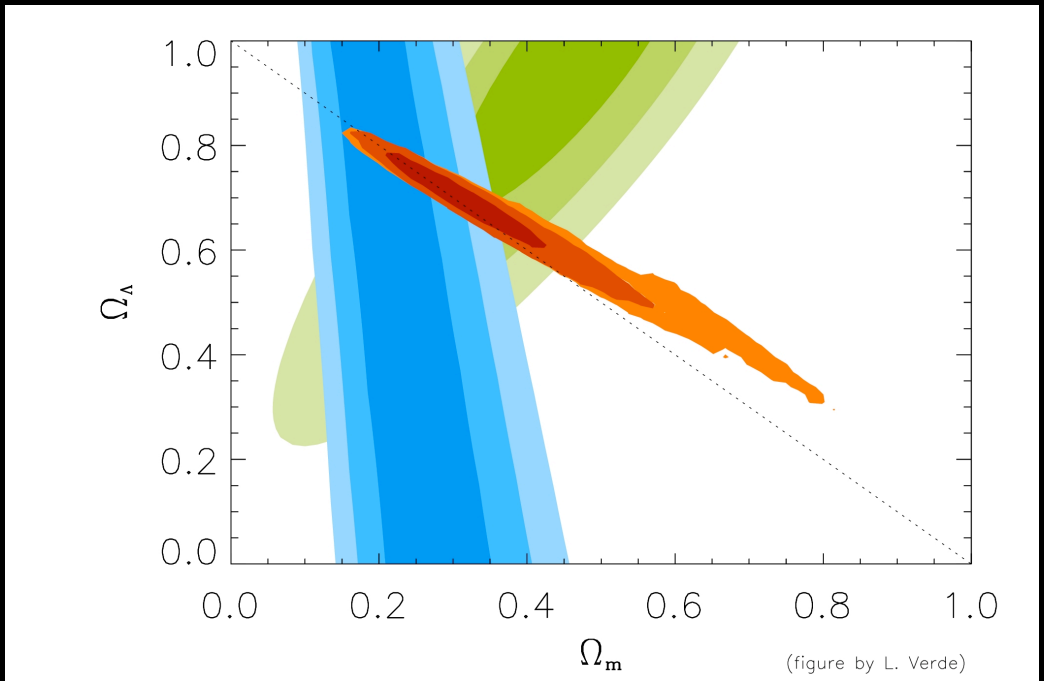

Perturbations: adiabatic

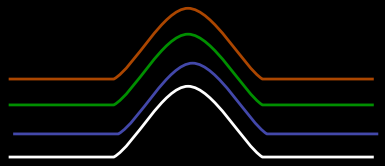

Photons
Neutrinos
Baryons(+electrons)
Dark matter
(dark energy negligible early on)

(isocurvature

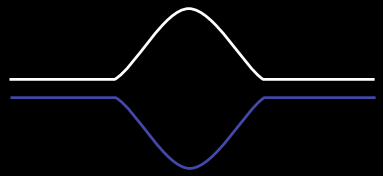

)

Tensor
(gravitational waves)

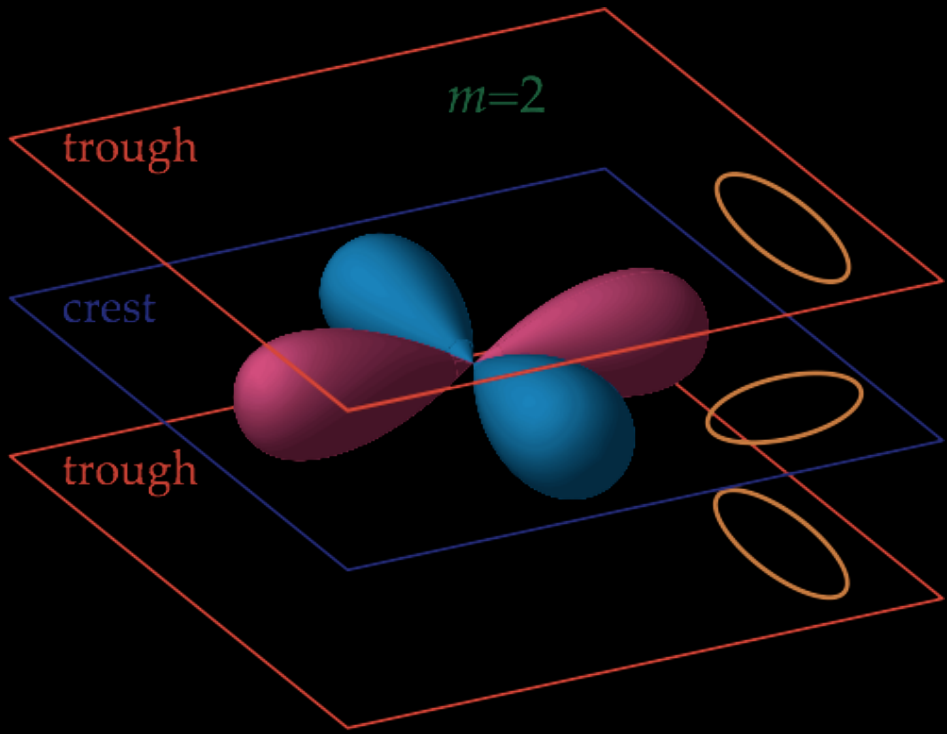

Fig. From W. Hu.

WMAP Consistent with Simplest Inflationary Models

- Flat universe: $\Omega_{tot} = 1.02 \pm 0.02$
- Gaussianity: $-58 < f_{NL} < 134$
- Power Spectrum spectral index nearly scale-invariant:
  $n_s = 0.99 \pm 0.04$ (*WMAP* only)
- Adiabatic initial conditions
- Superhorizon fluctuations (TE anticorrelations)

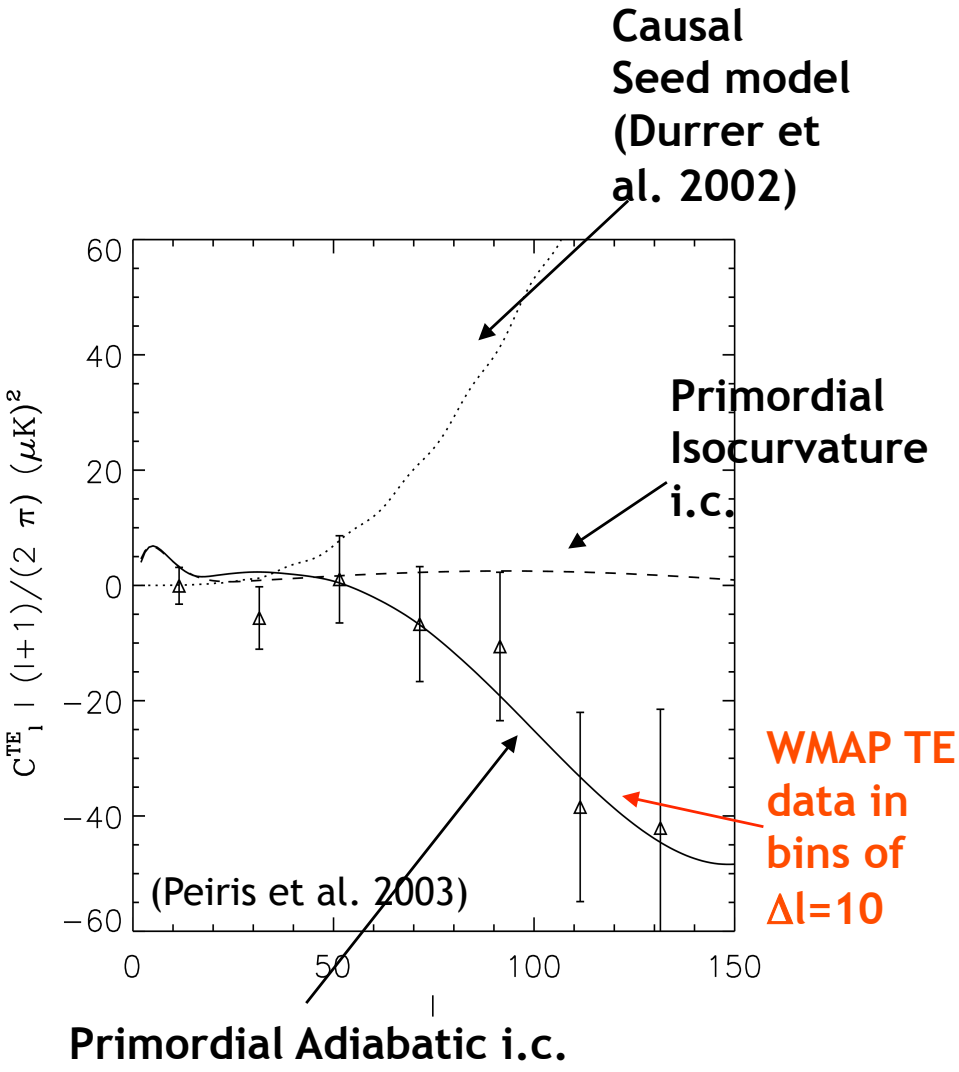

Hu & Sujiyama 1995
Zaldarriaga & Harari 1995
Spergel & Zaldarriaga 1997

Generation of CMB polarization

- Temperature quadrupole at the surface of last scatter generates polarization.

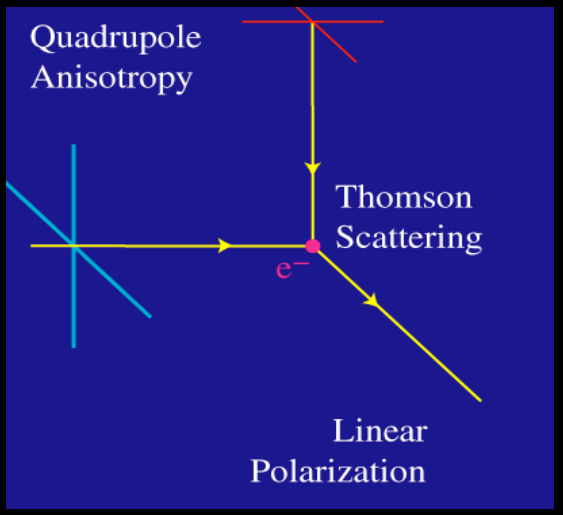

From Wayne Hu

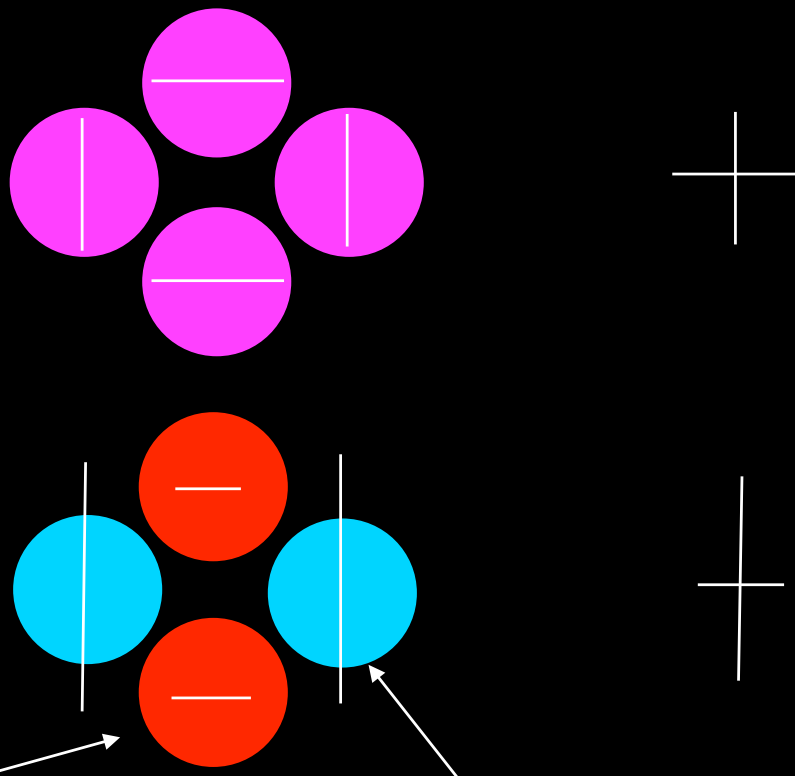

Polarization for density perturbation

- Radial (tangential) pattern around hot (cold) spots.

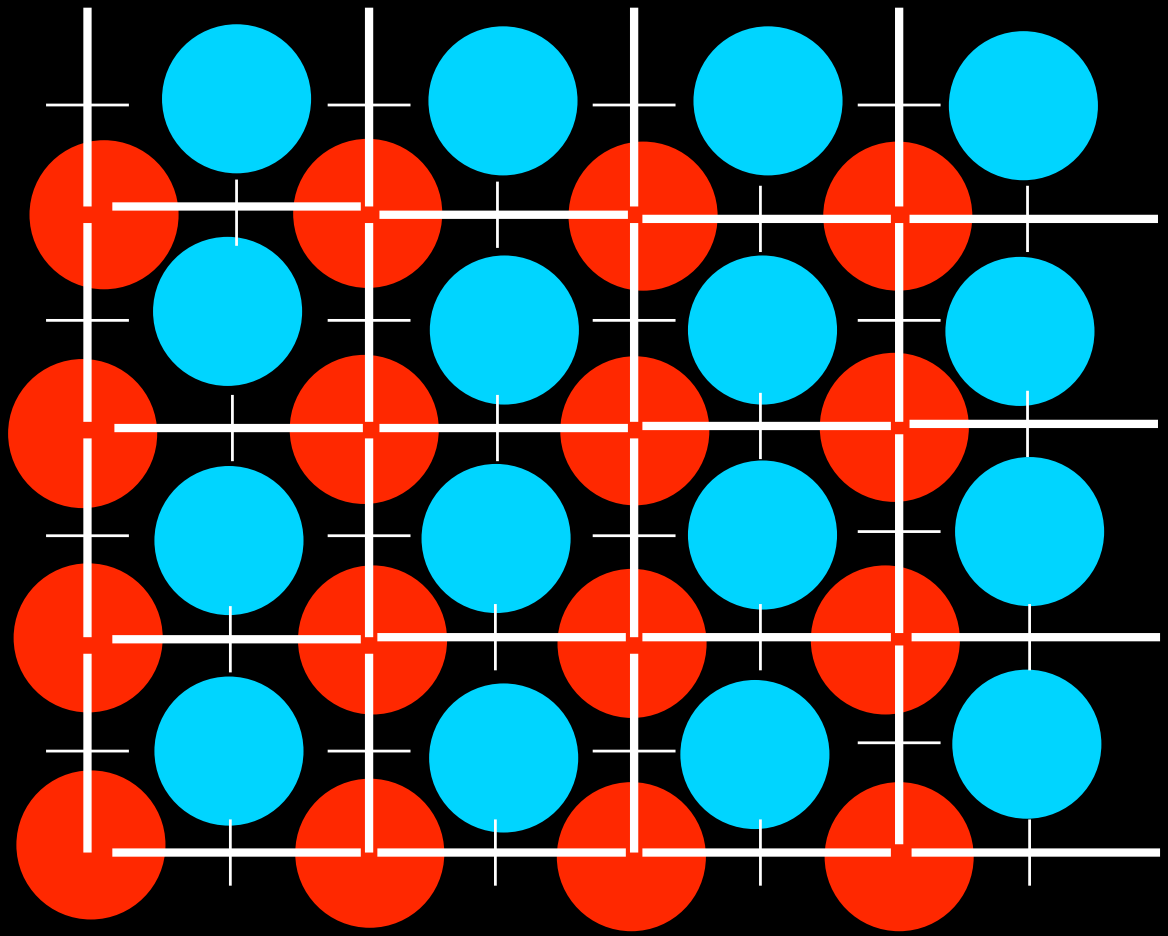

Gravity waves stretch space…

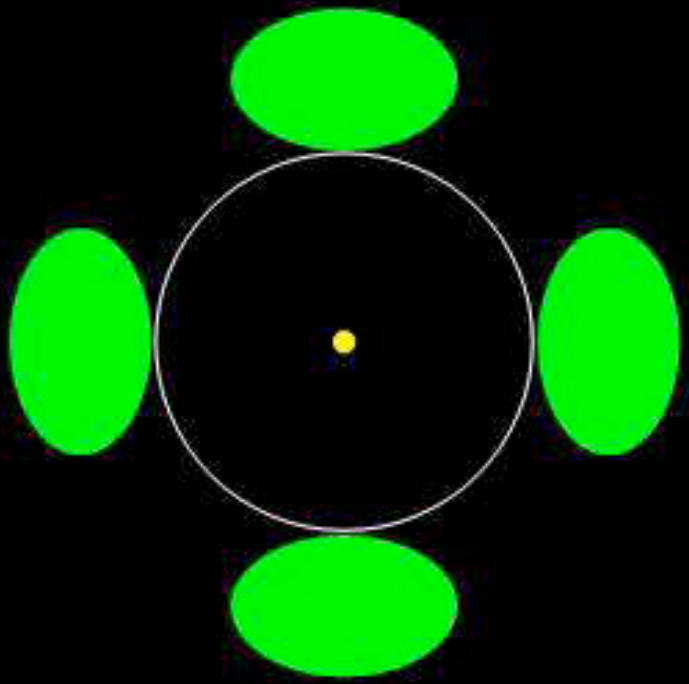

Image from J. Rhul.

… and create variations

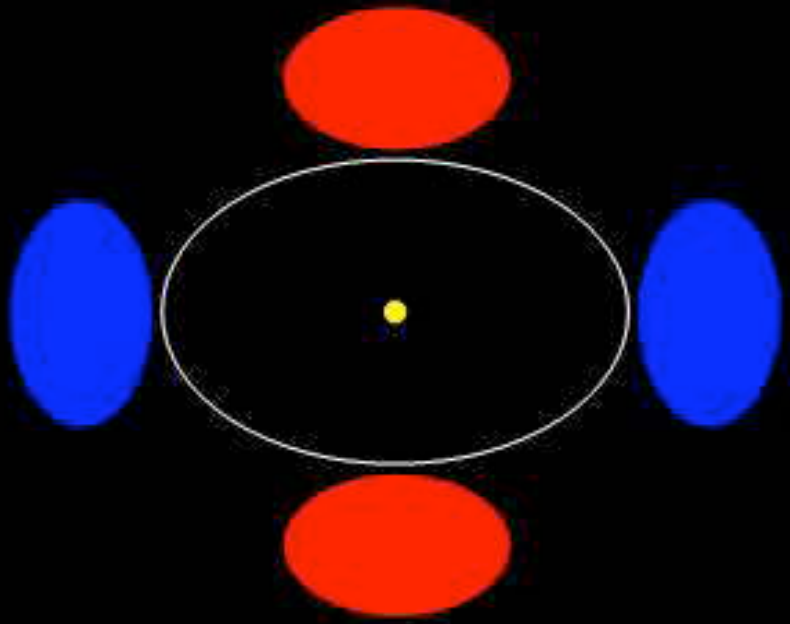

Image from J. Rhul.

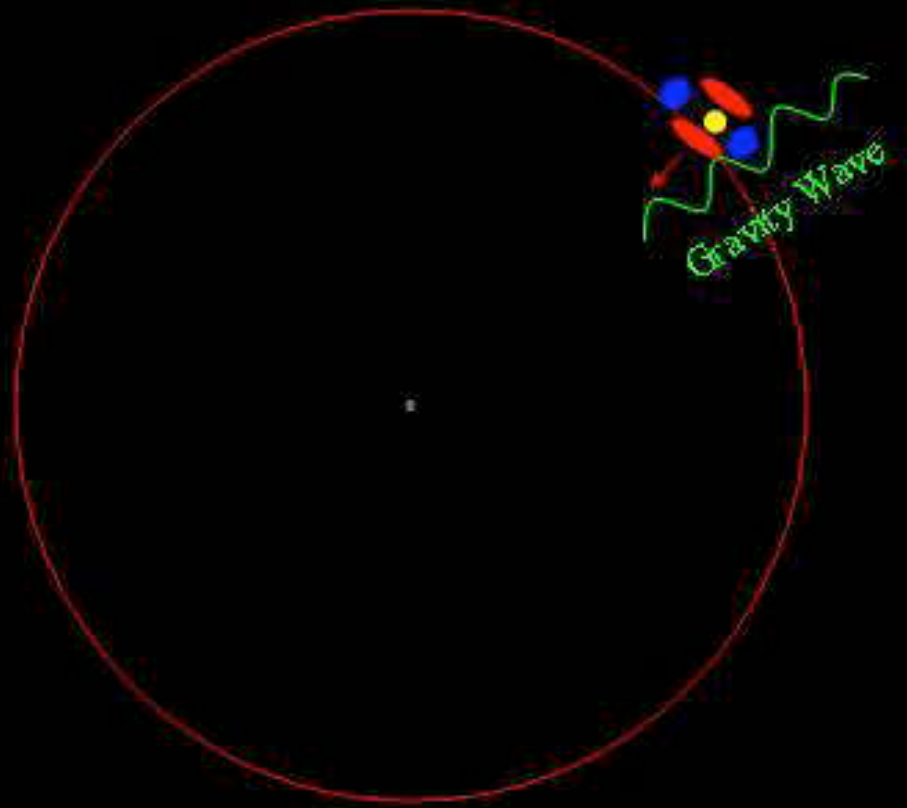
Gravity Wave

E and B modes polarization

E polarization
from scalar, vector and tensor modes

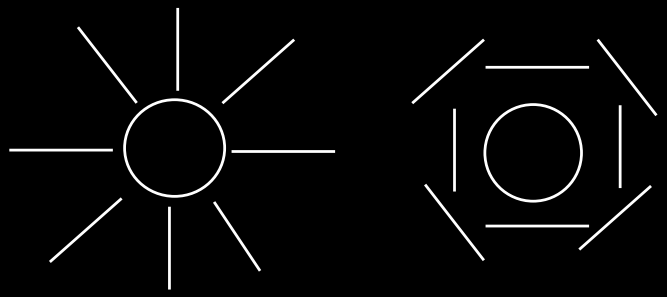

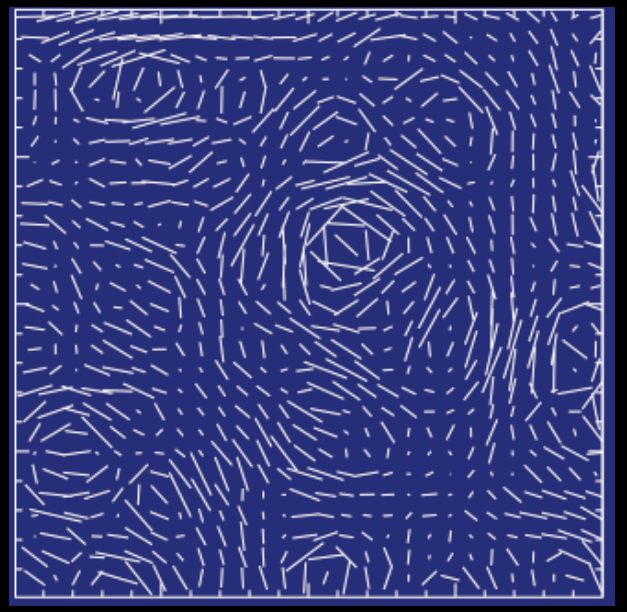

B polarization only from (vector)
tensor modes

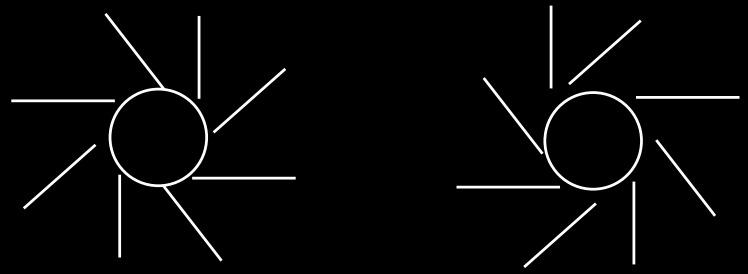

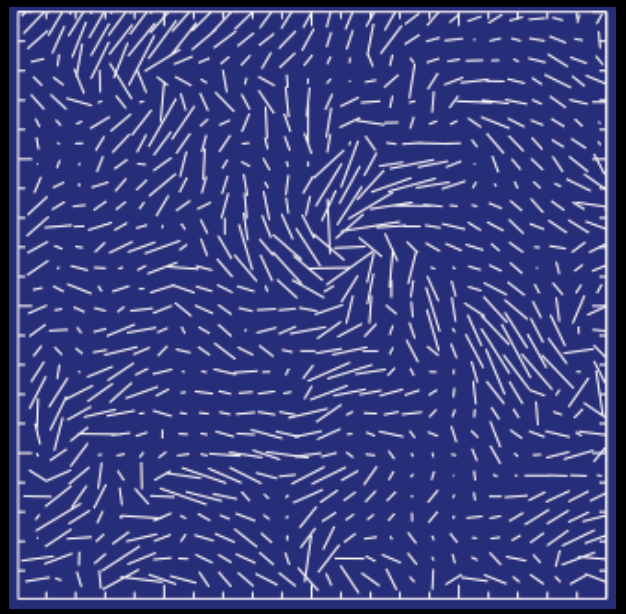

Kamionkowski, Kosowsky, Stebbings 1997, Zaldarriga & Seljak 1997

Gravity Waves in the CMB

Inflation produces two types of perturbations: in the energy density (as seen in TT) and in the gravitational field (gravity waves). Unlike temperature anisotropy, CMB polarization anisotropy can discriminate between scalar modes (density perturbations) and tensor modes (gravity waves). (r=tensor to scalar ratio)

1. Primordial B-mode anisotropy

- Inflation-generated gravity waves (tensor modes) polarize CMB
- (Kamionkowski & Kosowski 1998)
- A "smoking gun" of inflation => holy grail of CMB measurements
- At least an order of magnitude smaller than E-mode polarization
- Great experimental challenge: focus of this talk

2. Weak lensing B-modes (life is never easy…)

- Generated by weak lensing of the E-mode by large scale structure (Zaldarriaga & Seljak 1998)
- Subdominant on large scales, dominates on small scales

(Regular only)

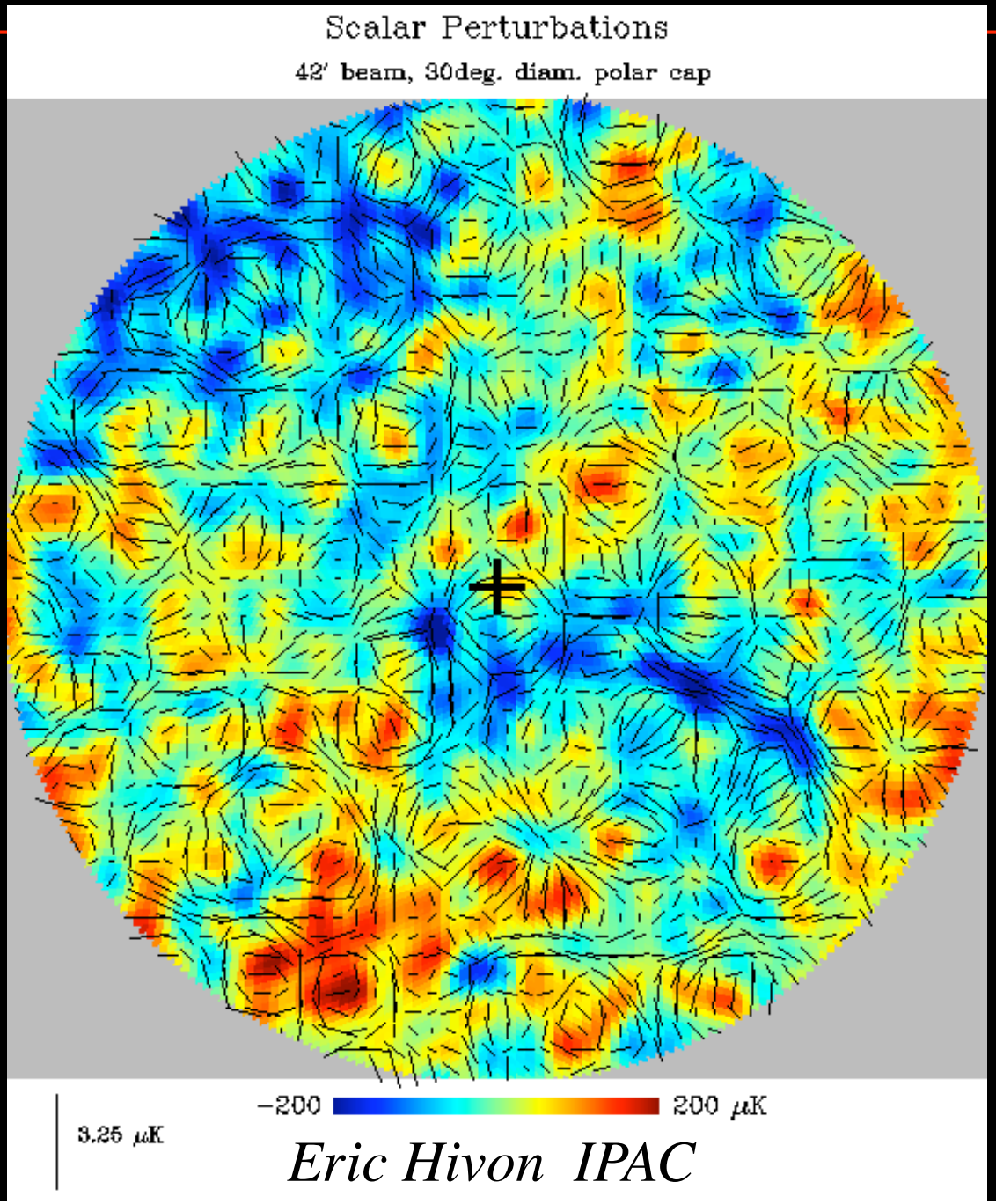

Eric Hivon IPAC

(Regular + Gravity waves)

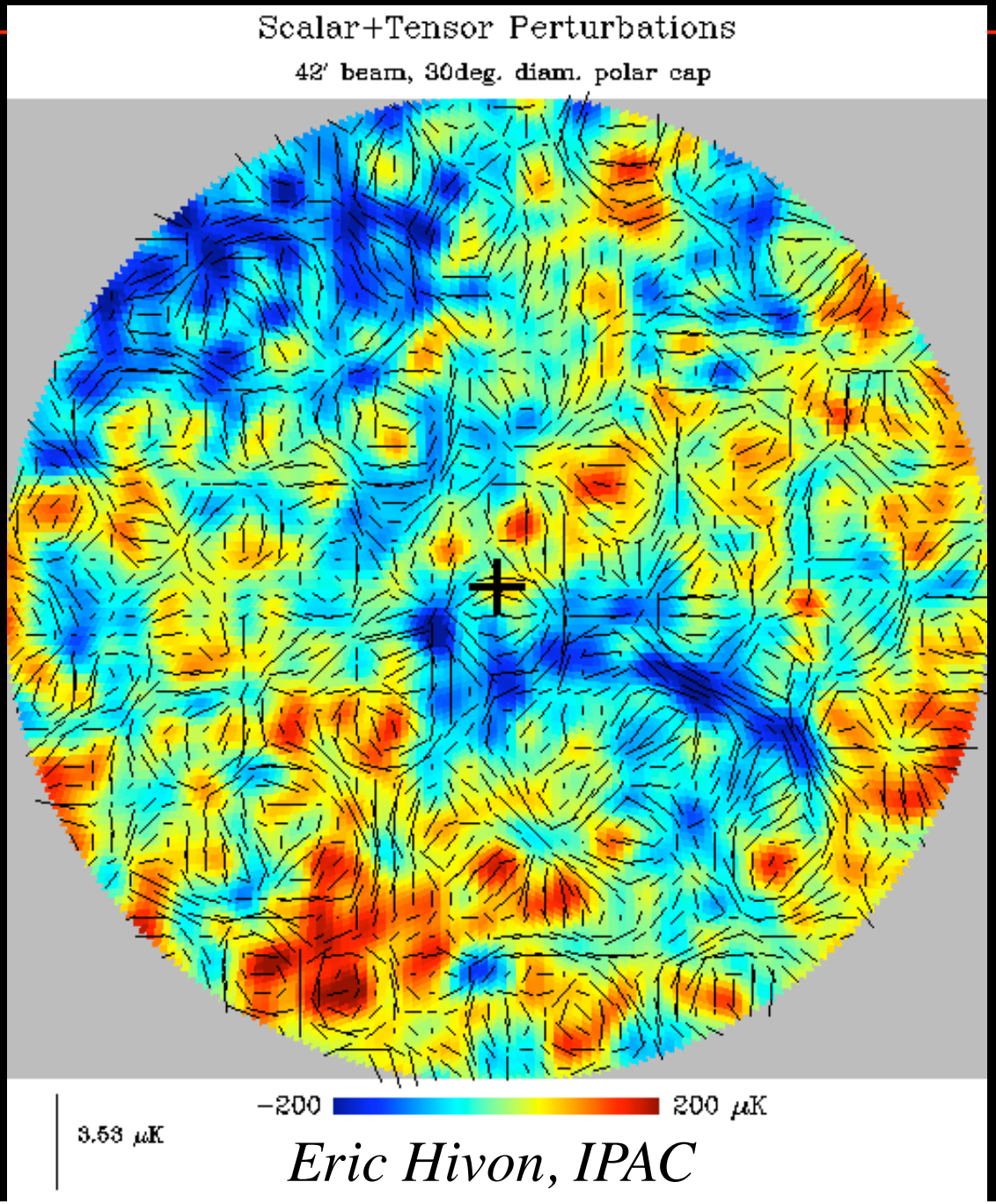

Eric Hivon, IPAC

Gravity Waves in the CMB

Inflation produces two types of perturbations: in the energy density (as seen in TT) and in the gravitational field (gravity waves). Unlike temperature anisotropy, CMB polarization anisotropy can discriminate between scalar modes (density perturbations) and tensor modes (gravity waves). (r=tensor to scalar ratio)

1. Primordial B-mode anisotropy

- Inflation-generated gravity waves (tensor modes) polarize CMB
- (Kamionkowski & Kosowski 1998)
- A "smoking gun" of inflation => holy grail of CMB measurements
- At least an order of magnitude smaller than E-mode polarization
- Great experimental challenge: focus of this talk

2. Weak lensing B-modes (life is never easy…)

- Generated by weak lensing of the E-mode by large scale structure (Zaldarriaga & Seljak 1998)
- Subdominant on large scales, dominates on small scales

Relative Amplitudes of CMB power spectra

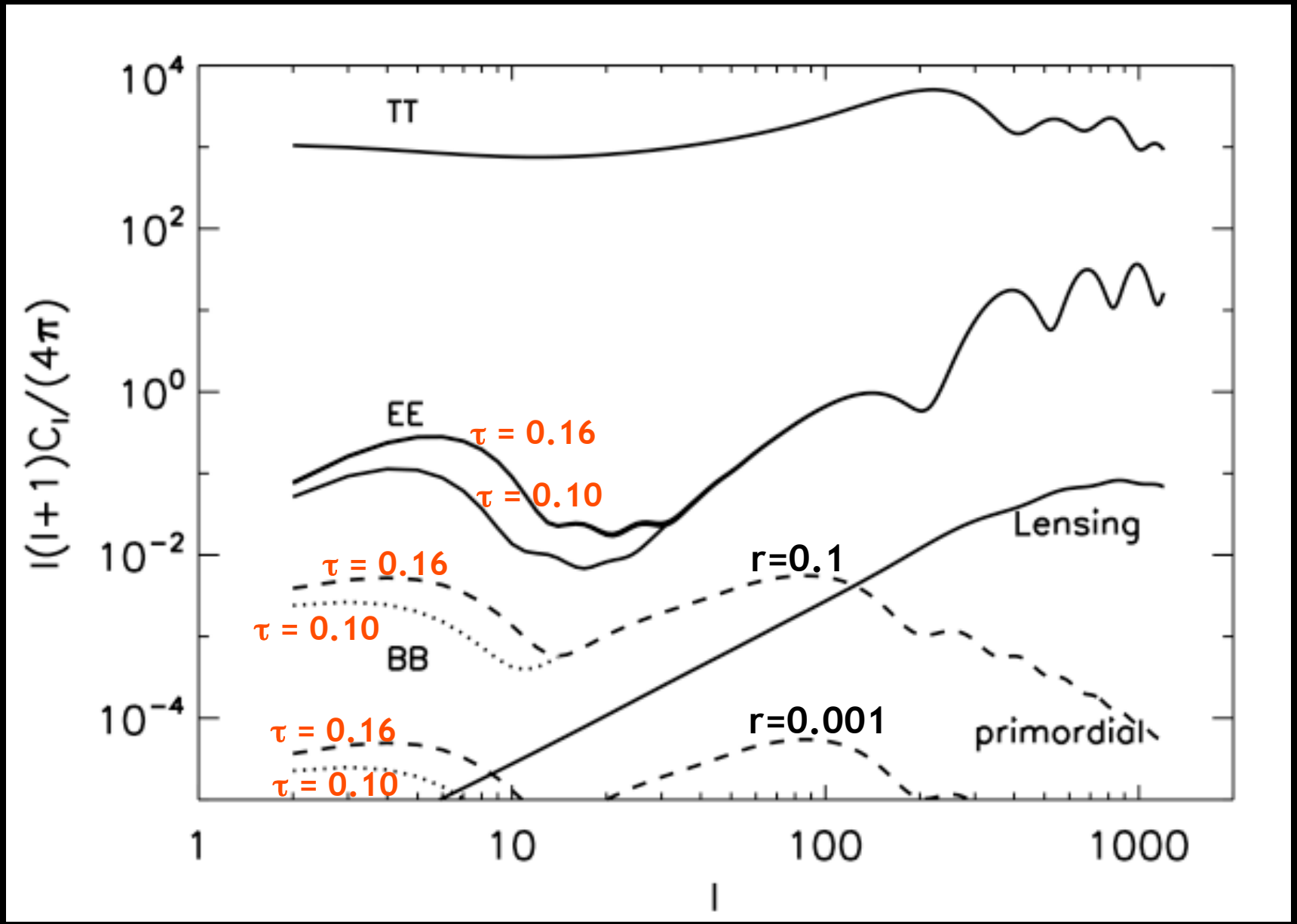

Obstacles to detecting and measuring B-modes

(it gets even worst…)

- **Fundamental complications:**
  - Level of primordial signal not guided at present by theory
  - Signal not significantly contaminated by lensing only on largest scales where cosmic variance is important
  - Polarized foreground emission on large scales likely dominate the signal at all frequencies

- **Practical complications:**
  - For signal to be detected in a reasonable timescale, instrumental noise needs to be well below the photon noise limit for a single detector ⇒ need multiple detectors
  - Polarized foregrounds not yet well known ⇒ foreground subtraction uncertainties seriously affect the goal

Relative Amplitudes of CMB power spectra

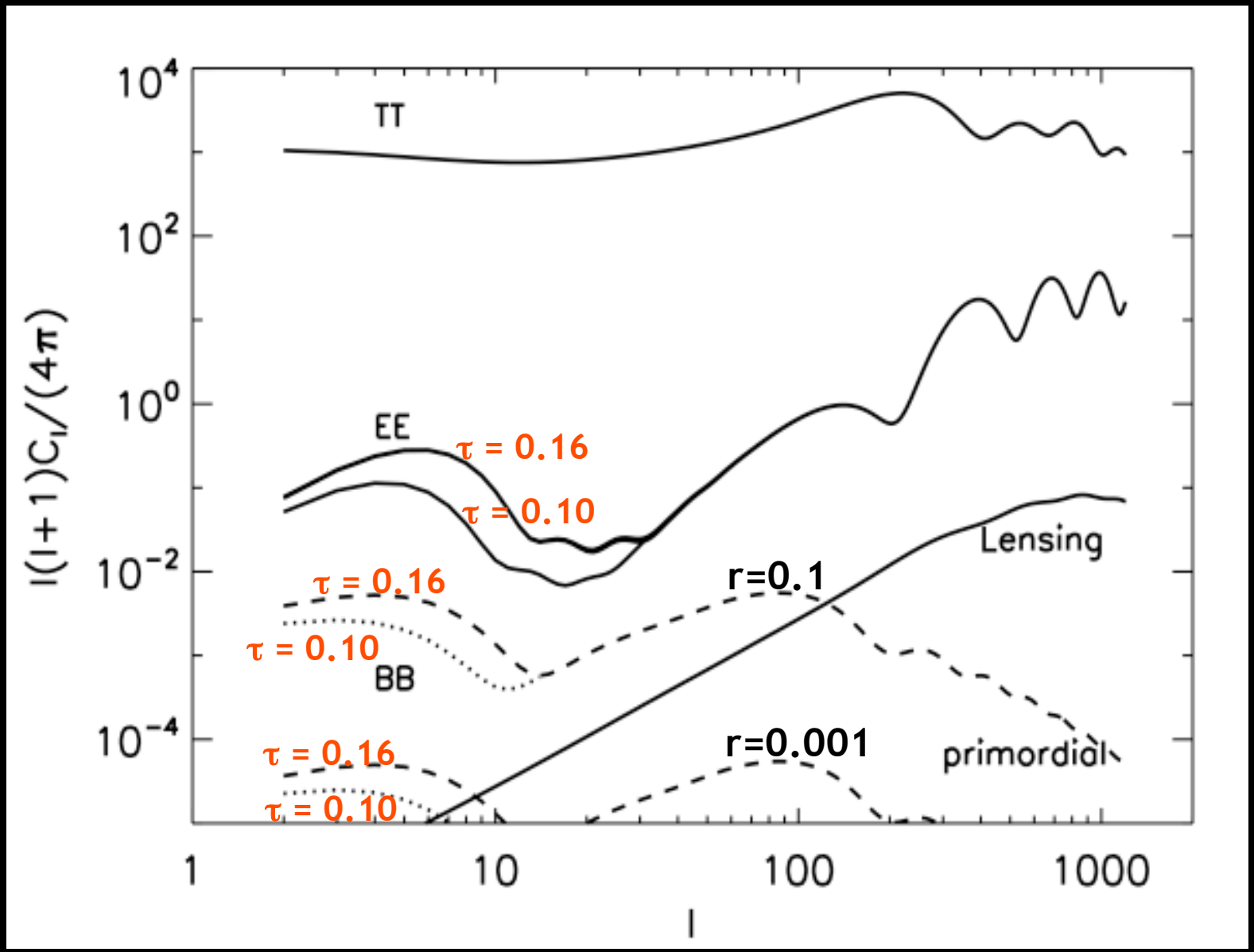

BB latest attempts

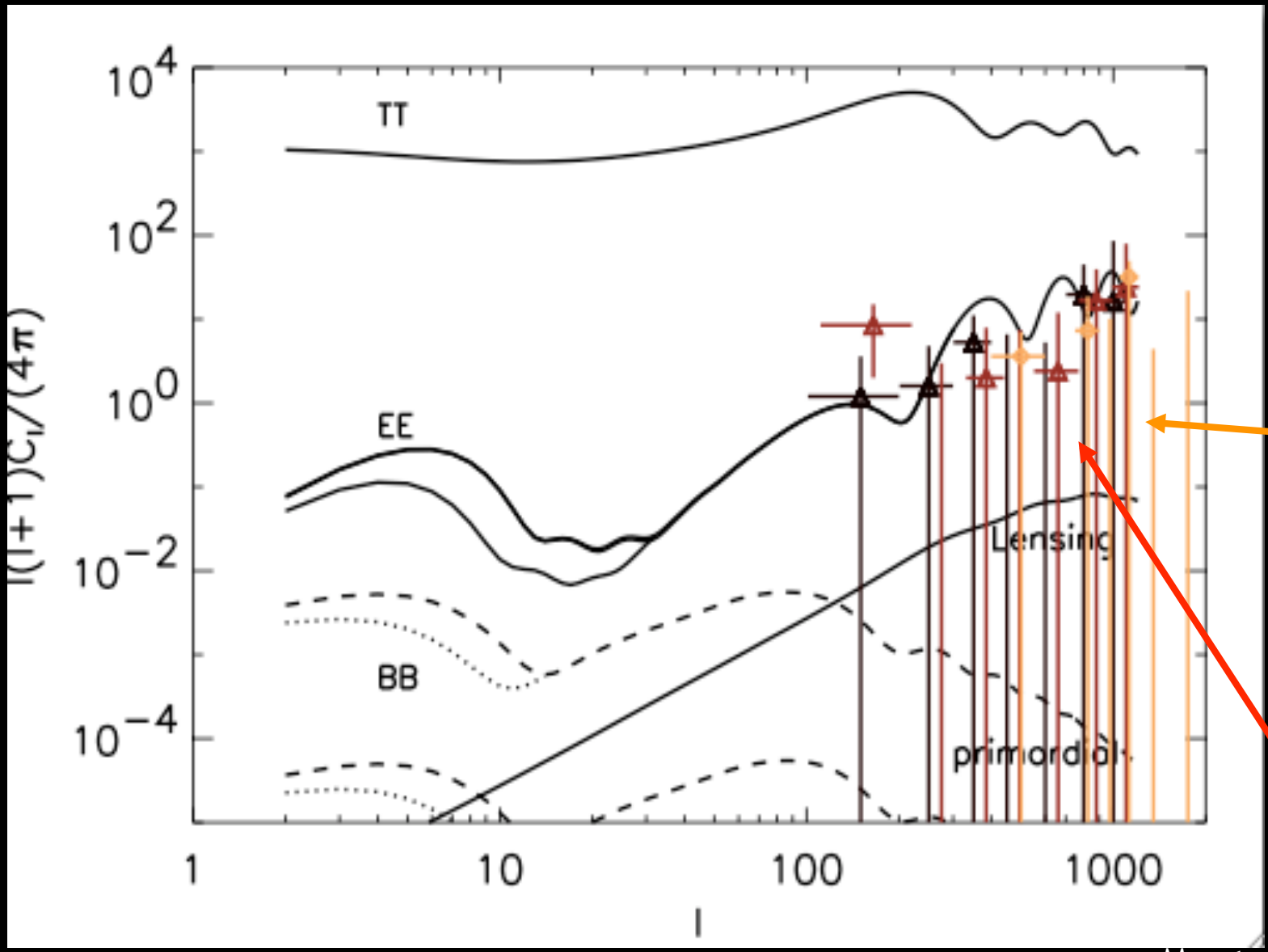

CBI,
Sievers
et al 2005

Boomerang
Montroy et al 05

Relative Amplitudes of CMB power spectra

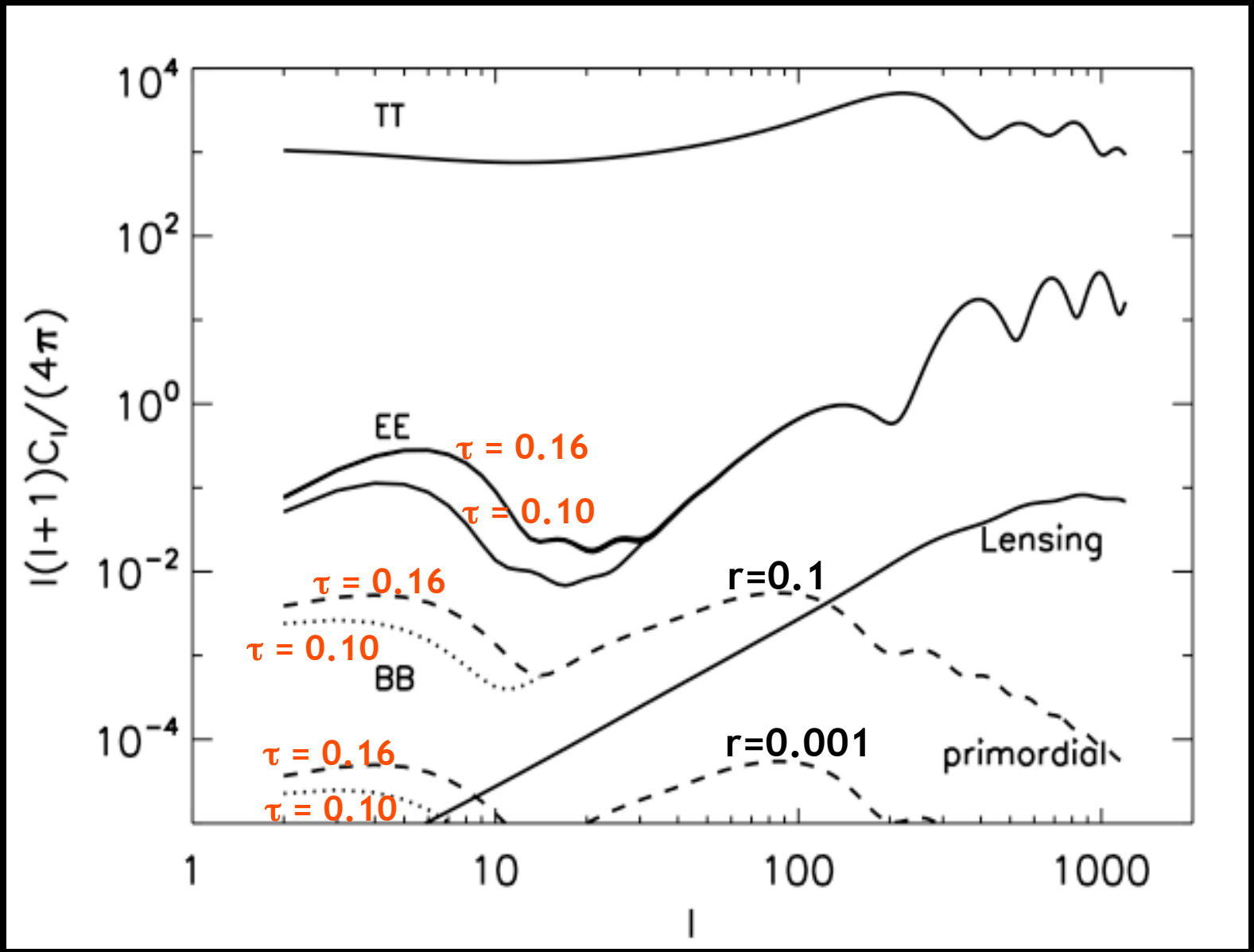

Foreground uncertainties vs CMB at l=4

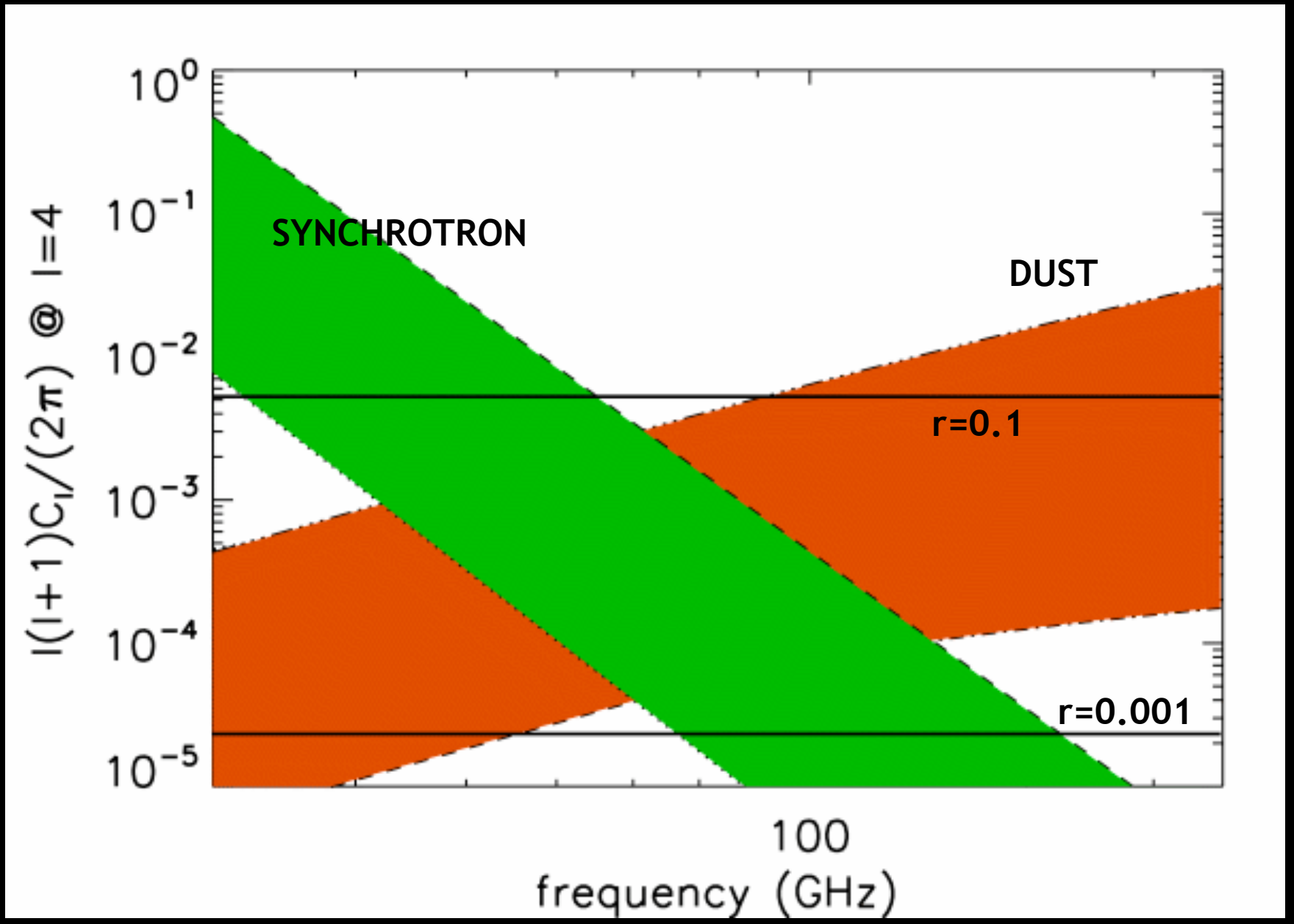

Foreground uncertainties vs CMB at l=80

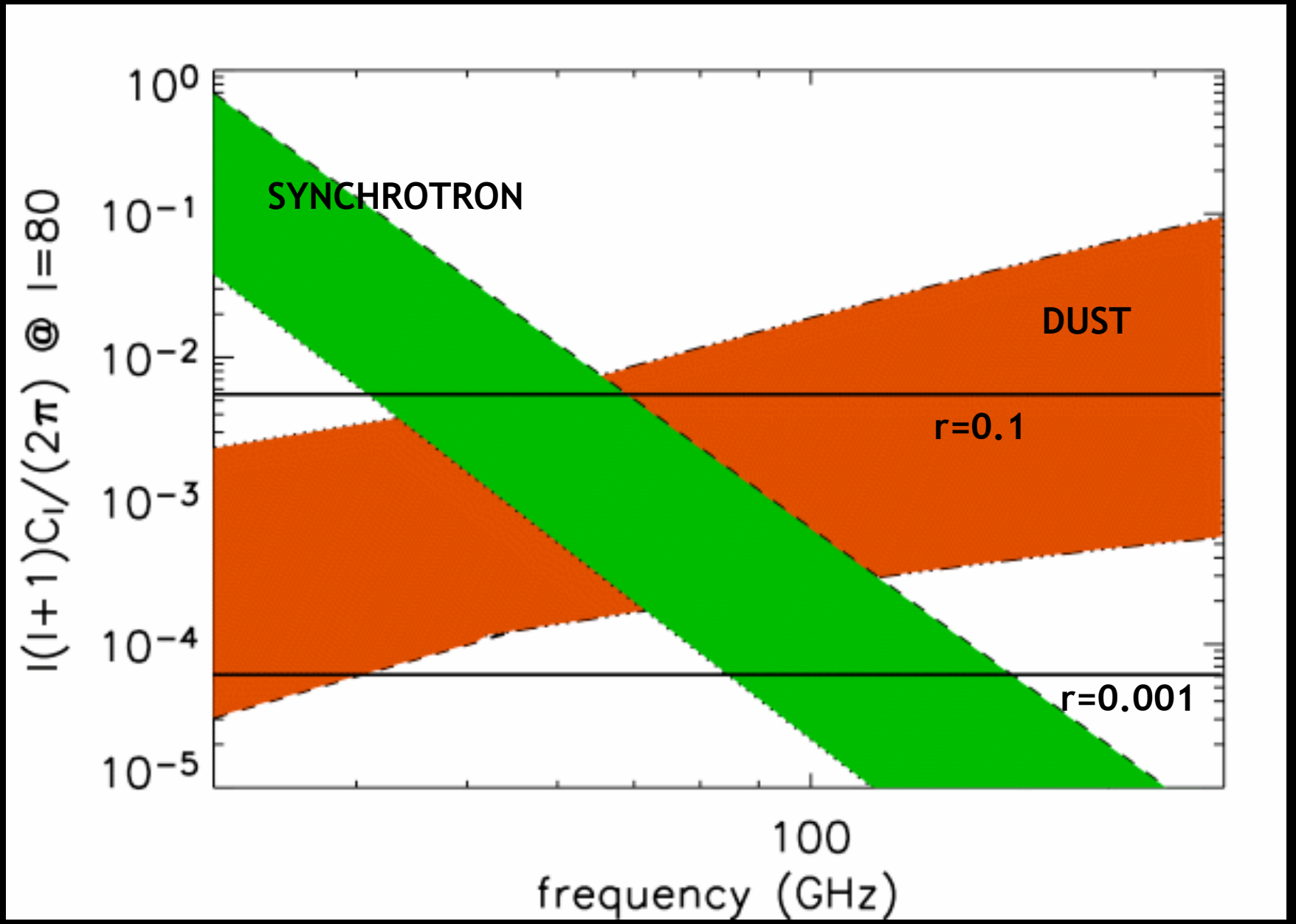

Purpose / Analysis Techniques

- **Attempt to forecast the performance of realistic next-generation CMB experiments(based on current technology):**
  - Space-based / ground-based / balloon-borne
  - Consider covariance between a full set of cosmological and primordial parameters (with/without imposing flatness and consistency relation)
  - Consider effects of foreground contamination, instrumental noise and partial sky coverage: what is the limiting factor?
  - What is the point of diminishing returns in increasing number of detectors to decrease noise, and increasing number of channels to improve foreground cleaning?
- **Consider what these realistic forecasts can tell us about inflation.**

Analysis Technique

Fisher matrix approach:

$$
\begin{aligned}
-2\ln\mathcal{L} &= \sum_{\ell}(2\ell+1)\left\{ f_{sky}^{BB}\ln\left(\frac{\mathbf{C}_\ell^{BB}}{\hat{\mathbf{C}}_\ell^{BB}}\right)\right. \\
&+ \sqrt{f_{sky}^{TT}f_{sky}^{EE}}\ln\left(\frac{\mathbf{C}_\ell^{TT}\mathbf{C}_\ell^{EE}-(\mathbf{C}_\ell^{TE})^2}{\hat{\mathbf{C}}_\ell^{TT}\hat{\mathbf{C}}_\ell^{EE}-(\hat{\mathbf{C}}_\ell^{TE})^2}\right) \\
&+ \sqrt{f_{sky}^{TT}f_{sky}^{EE}}\frac{\hat{\mathbf{C}}_\ell^{TT}\mathbf{C}_\ell^{EE}+\mathbf{C}_\ell^{TT}\hat{\mathbf{C}}_\ell^{EE}-2\hat{\mathbf{C}}_\ell^{TE}\mathbf{C}_\ell^{TE}}{\mathbf{C}_\ell^{TT}\mathbf{C}_\ell^{EE}-(\mathbf{C}_\ell^{TE})^2} \\
&+ \left. f_{sky}^{BB}\frac{\hat{\mathbf{C}}_\ell^{BB}}{\mathbf{C}_\ell^{BB}}-2\sqrt{f_{sky}^{TT}f_{sky}^{EE}}-f_{sky}^{BB}\right\} \qquad (15)
\end{aligned}
$$

$$F_{ij} = \left\langle -\frac{\partial^2 L}{\partial\alpha_i\alpha_j}\right\rangle|_{\alpha=\bar{\alpha}}$$

Covariance : $\mathbf{S_{ij}=F^{-1}}_{ij}$

$$\mathbf{C}_\ell^{XY} = C_\ell^{XY} + \mathcal{N}_\ell^{XY}$$

What about foregrounds?

Foregrounds: Synchrotron

$$C_\ell^{S,XY} = A^S \left(\frac{\upsilon}{30\,\mathrm{GHz}}\right)^{2\alpha_S} \left(\frac{\ell}{300}\right)^{\beta_S}$$

Information about polarized synchrotron is limited at present to frequencies much lower than CMB and mostly low Galactic latitudes, and show spatial and frequency variations.

We assume $\alpha_S = -3$ e.g. Platania et al. (1998, 2003; Bennett et al. (2003) and $\beta_S = -1.8$ e.g. Baccigalupi et al. (2001); Bruscoli et al. (2002); Bernardi et al. (2003, 2004) for both E and B.

A^S is set by

- Pessimistic case: DASI 95% upper limit 0.91 μK^2 Leitch et al (2005)
- Reasonable case: 50% of DASI limit
- Optimistic case: 10% of DASI limit (only for partial sky experiments looking at clean patch) c.f. Carretti et al. (2005)

Foregrounds: Dust

$$C_\ell^{D,XY} = p^2 A^D \left(\frac{\upsilon}{94\,\mathrm{GHz}}\right)^{2\alpha_D} \left(\frac{\ell}{900}\right)^{\beta_D{}^{XY}} \left[\frac{e^{h(94\,\mathrm{GHz})/kT} - 1}{e^{h\upsilon/kT} - 1}\right]^2$$

Assume temperature of dust grains to be a uniform 18 K across sky.

We assume $\alpha_D = 2.2$ Bennett et al. (2003). Archeops finds $\alpha_D = 1.7$; with our choice, extrapolation to higher frequencies more conservative.

$\beta_D{}^{EE} = -1.3$, $\beta_D{}^{BB} = -1.4$, $\beta_D{}^{TE} \sim -1.95$, $\beta_D{}^{TT} \sim -2.6$ Lazarian and Prunet (2002); Prunet et al. (1998) (in agreement with the measurement of starlight polarization of Fosalba et al (2002)).

A^D is set by the intensity normalization of Finkbeiner et al. (1999) extrapolated to 94 GHz.

Polarization fraction p=5% set by Archeops upper limit Benoit et al. (2004); p=1% lower limit (3 μG weak Galactic field Padoan et al. 2001).

Fiducial Foregrounds vs CMB at 70 GHz

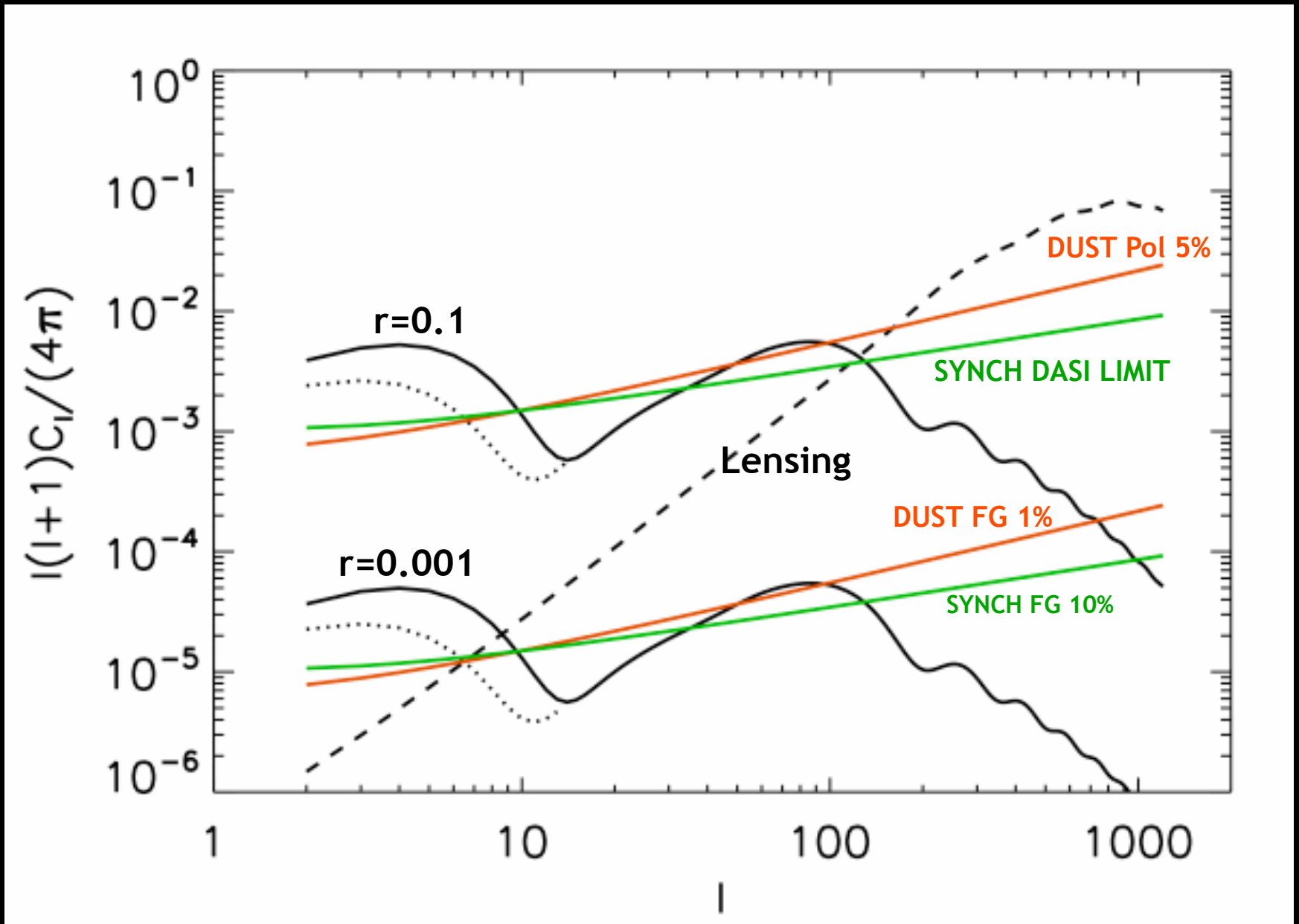

Propagation of FG subtraction errors

Assume FG subtracted from maps via FG templates or MEM techniques.

$$C_\ell^{res,fg,XY}(\upsilon) = C_\ell^{fg,XY}(\upsilon)\,\sigma^{fg,XY} + N^{fg,XY}\left(\frac{\upsilon}{\upsilon_{template}}\right)^{-2\langle\alpha_{fg}\rangle}$$

Residual contamination

FG power spectrum

Fraction of FG left after subtraction

Noise PS of template map

Template freq.

Avg value of spectral index

The template freq. assumed to coincide with the experimental channel where contamination is highest for that component.

c.f. result of Tucci et al (2004)

Delensing

•Delensing techniques exploit non-Gaussianity of lensed CMB, but FG expected to be highly non-Gaussian (reconstruction techniques not explored in their presence).

•If FG neglected, assume delensing can only be implemented in signal-dominated regime; can only reduce BB-lensing signal to instrumental noise level. c.f. result of Hirata and Seljak (2003)

•If FG included, assume delensing can be applied only if FG emission + template noise power spectrum is 10% of BB-lensing signal, and BB-lensing signal can only be reduced down to 10% of FG signal (emission+template noise).

•For realistic case with noise and FG, find delensing can be implemented if an experiment can be carefully designed to achieve low noise, 1% FG cleaning and observe a relatively clean patch of sky.

Next Generation Observational Prospects

- Space-based
  - Planck l~3000 (k~0.2/Mpc)
  - CMBPol/Inflation Probe?
- Ground-based
  - e.g. BICEP, CLOVER, PolarBeaR , QuAD, QUIET
- Balloon-borne
  - SPIDER, EBEX

Next Generation Observational Prospects

- Space-based
  - Planck l~3000 (k~0.2/Mpc)
  - CMBPol/Inflation Probe?
- Ground-based
  - e.g. BICEP, CLOVER, PolarBeaR , QuAD, QUIET
- Balloon-borne
  - SPIDER, EBEX

Considerations about detectors

PolarBeaR: Polarization-sensitive array of bolometers

(Good above ~100 GHz. E.g. Boomerang, DASI)

Limited by photon shot noise

QUIET: HEMT polarimeters

(good below ~ 100 GHz. WMAP uses HEMT technology)

$$\Delta T_{rms} = \frac{T_{CMB} + T_{receiver}}{\sqrt{\Delta\nu\Delta t}}$$

Detector arrays needed to beat the noise limit per detector

Wide frequency range needed to keep foregrounds in check

Heavy!

Low l's are Lensing-free → Large sky coverage → Space

Weigh restrictions!

Summary of experimental characteristics

	frequency (GHz)	noise/beam (μK)	beam FWHM ($'$)	sky coverage (f_{sky} or sq. deg.)
SAT	30, 50, 70, 100, 200	2.2 per channel	8	f_{sky}=0.8
QUIET	40	0.43	23	4 × 400
	90	0.78	10	
PolarBeaR	90	1.6	6.7	500
	150	2.4	4.0	
	220	11.3	2.7	
QUIET+PolarBeaR	40	0.43	23	400
	90	0.78	10	
	90	1.6	6.7	
	150	2.4	4.0	
	220	11.3	2.7	
QUIETBeaR *	40	0.1	23	170
	90	0.18	10	
	90	0.18	10	
	150	0.18	10	
	220	0.18	10	
SPIDER	40	0.74	145	f_{sky}=0.4
	84	0.36	69	
	92	0.36	63	
	100	0.36	58	
	145	0.58	40	
	220	1.6	26	

SAT frequency coverage

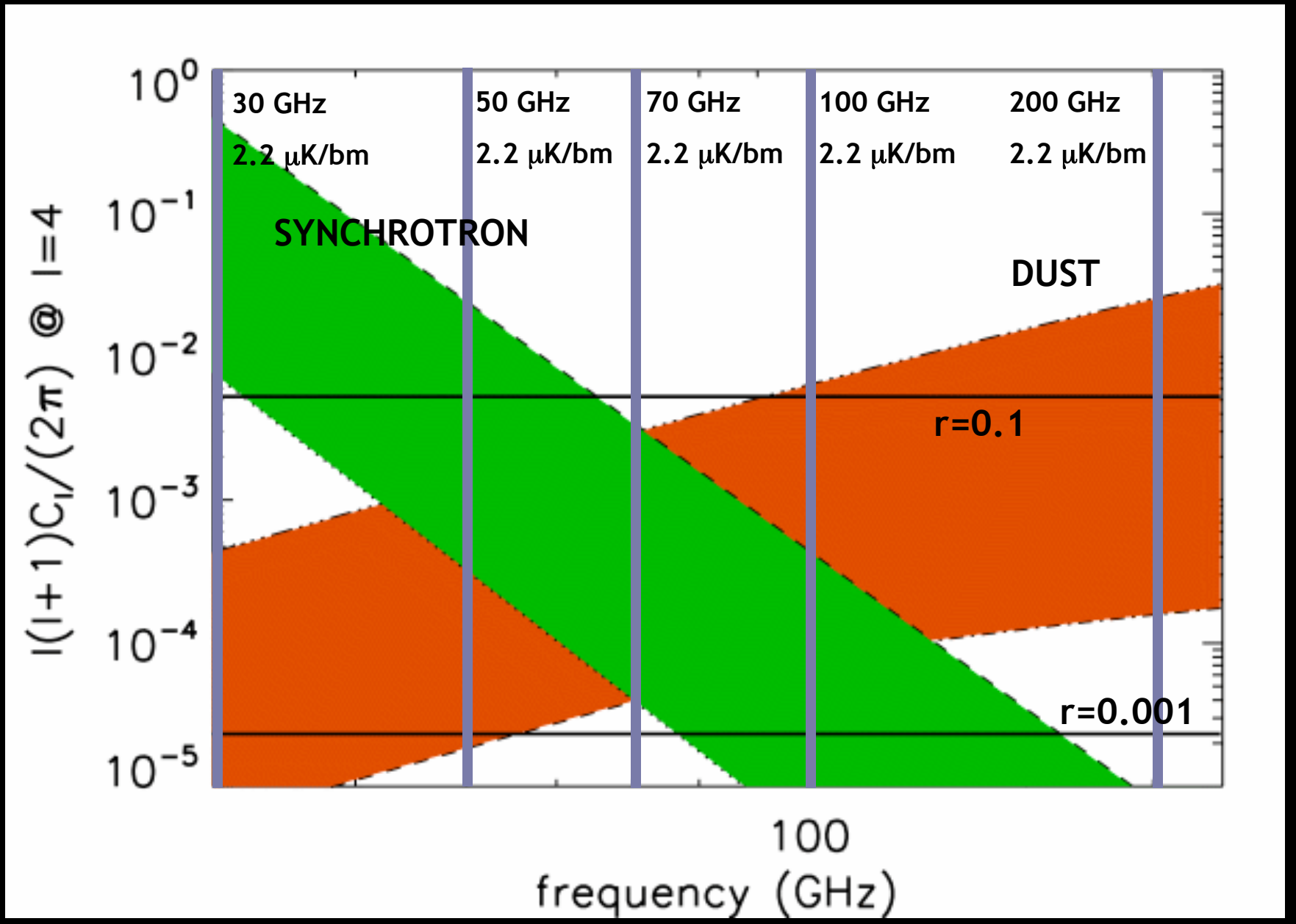

SPIDER frequency coverage

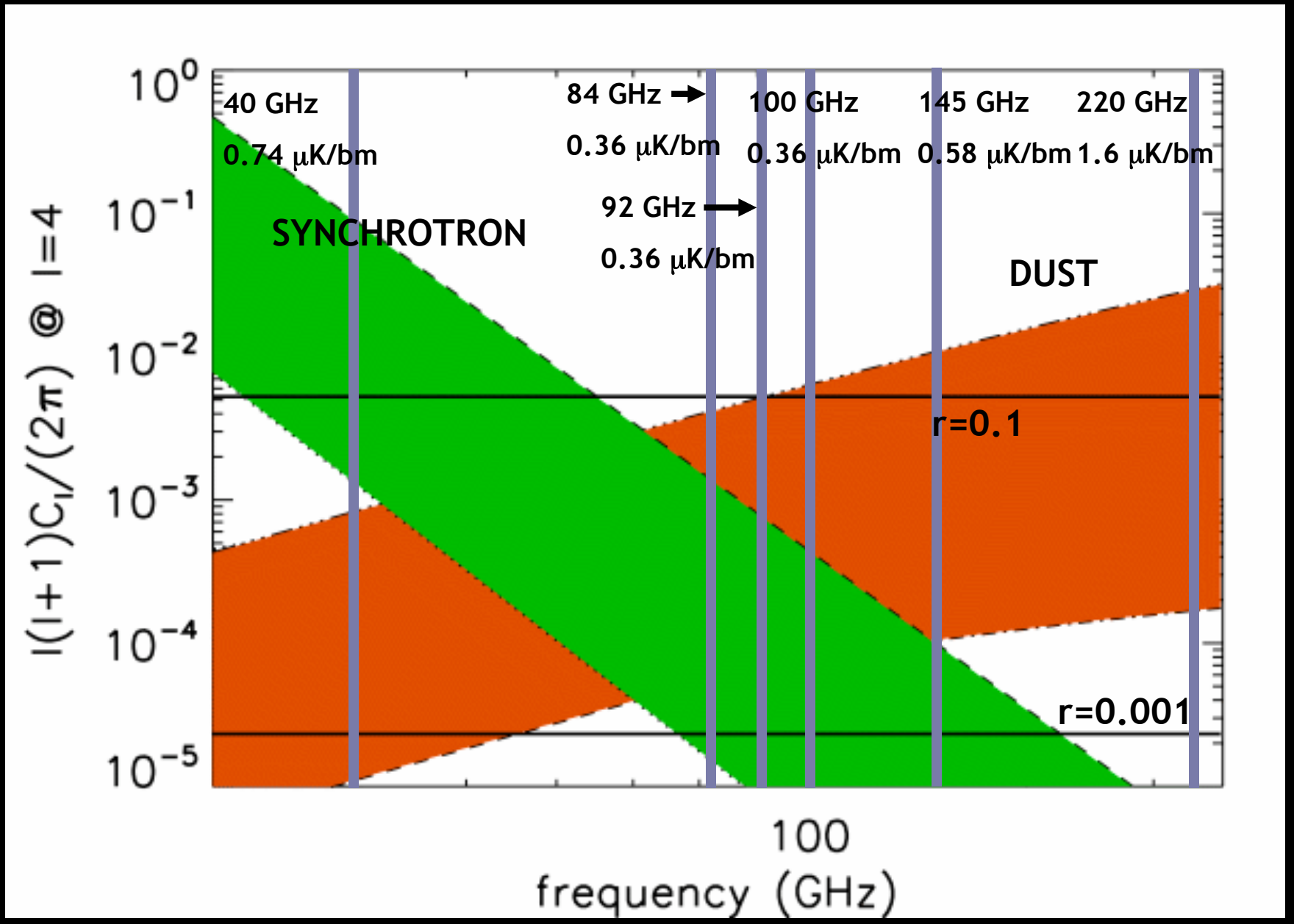

QUIET frequency coverage

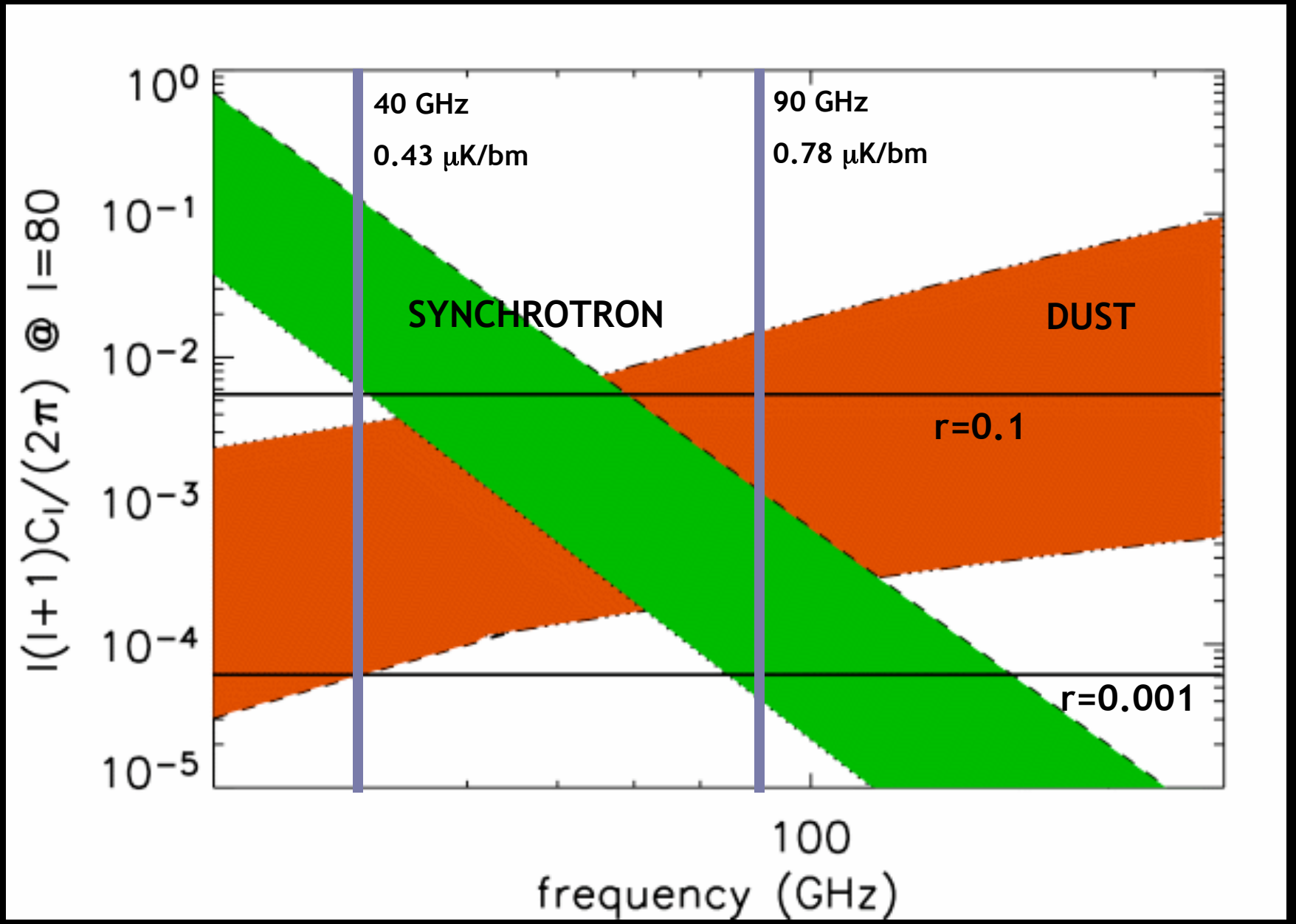

PolarBeaR frequency coverage

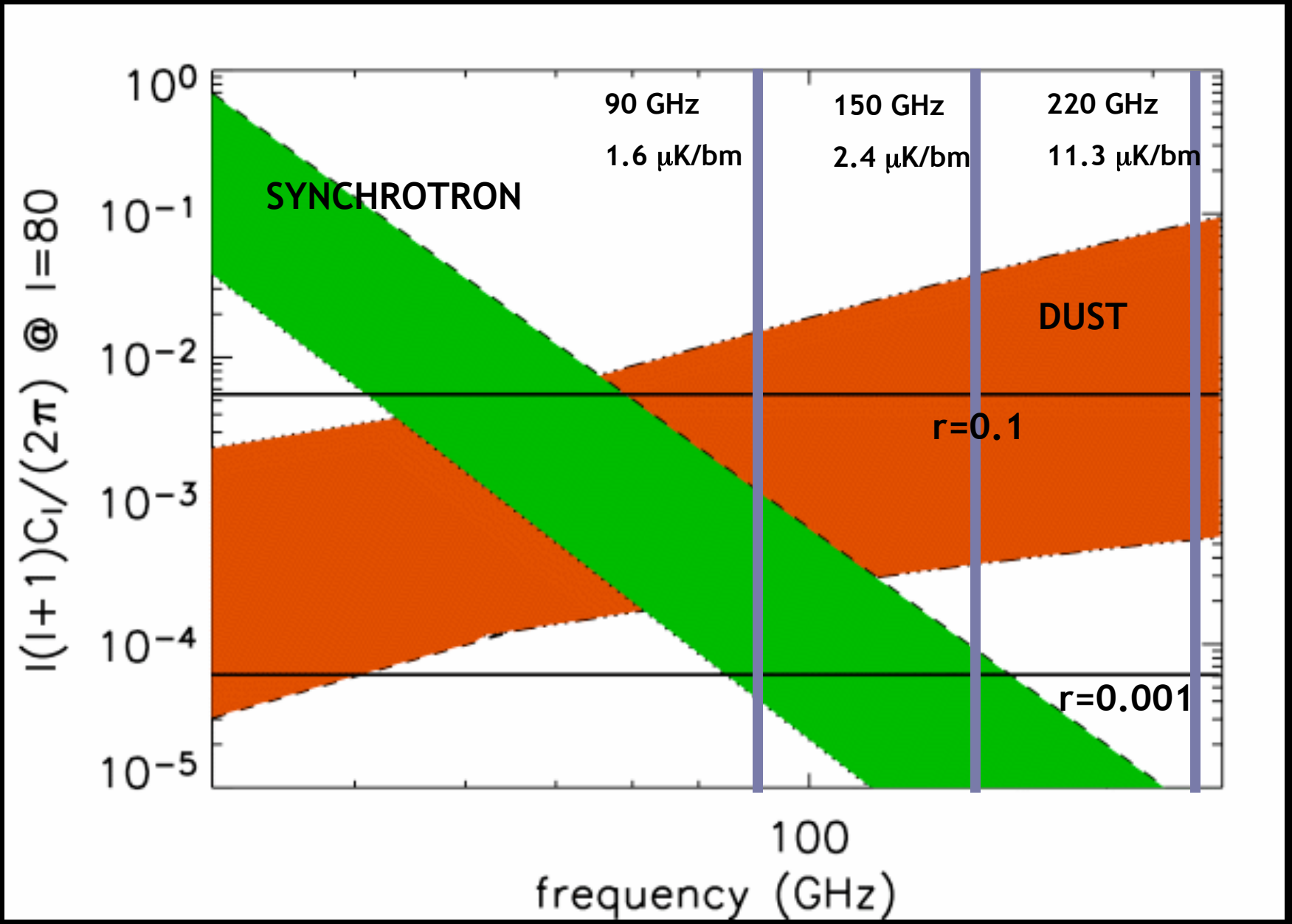

QUIET+PolarBeaR frequency coverage

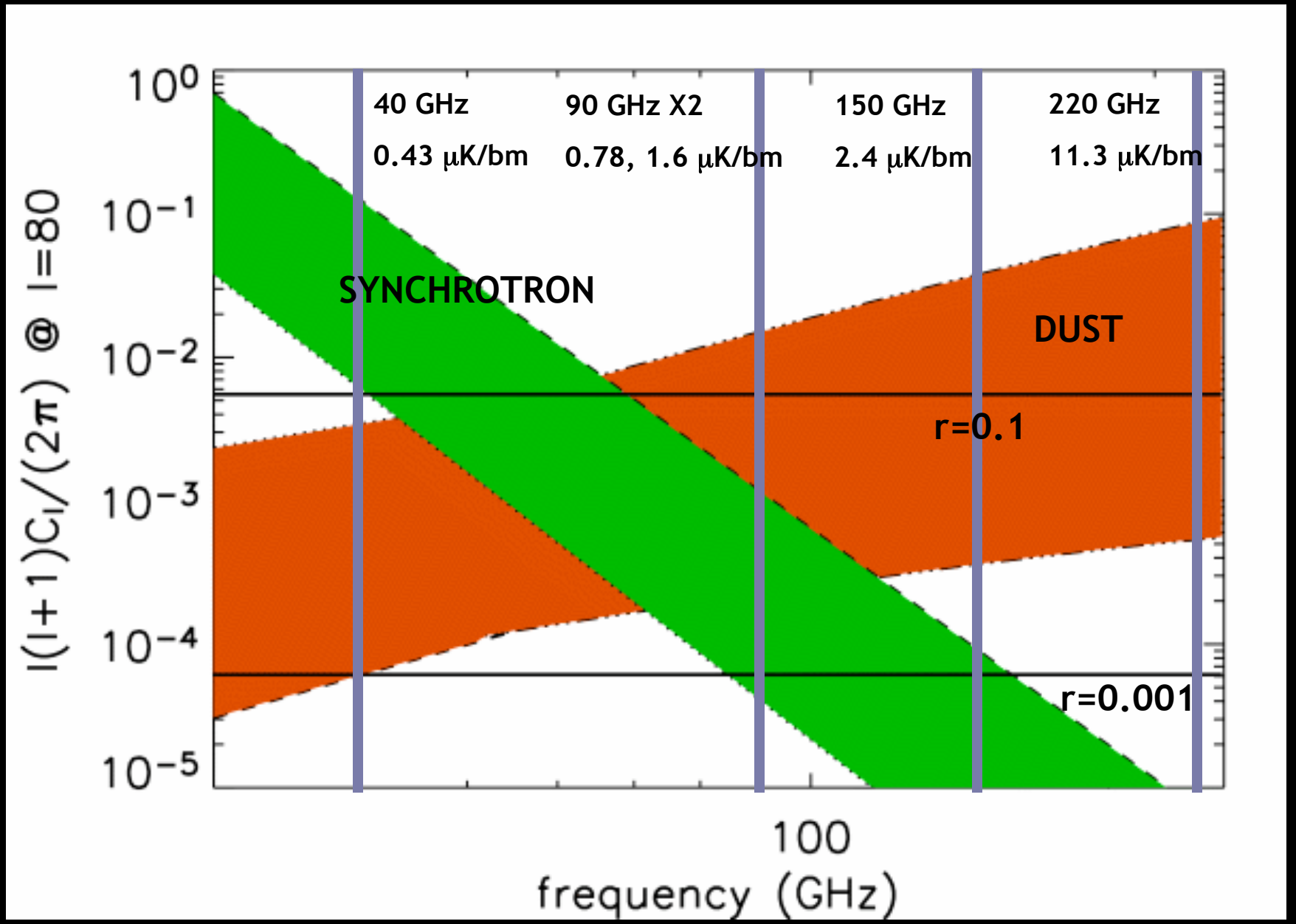

QUIETBeaR frequency coverage

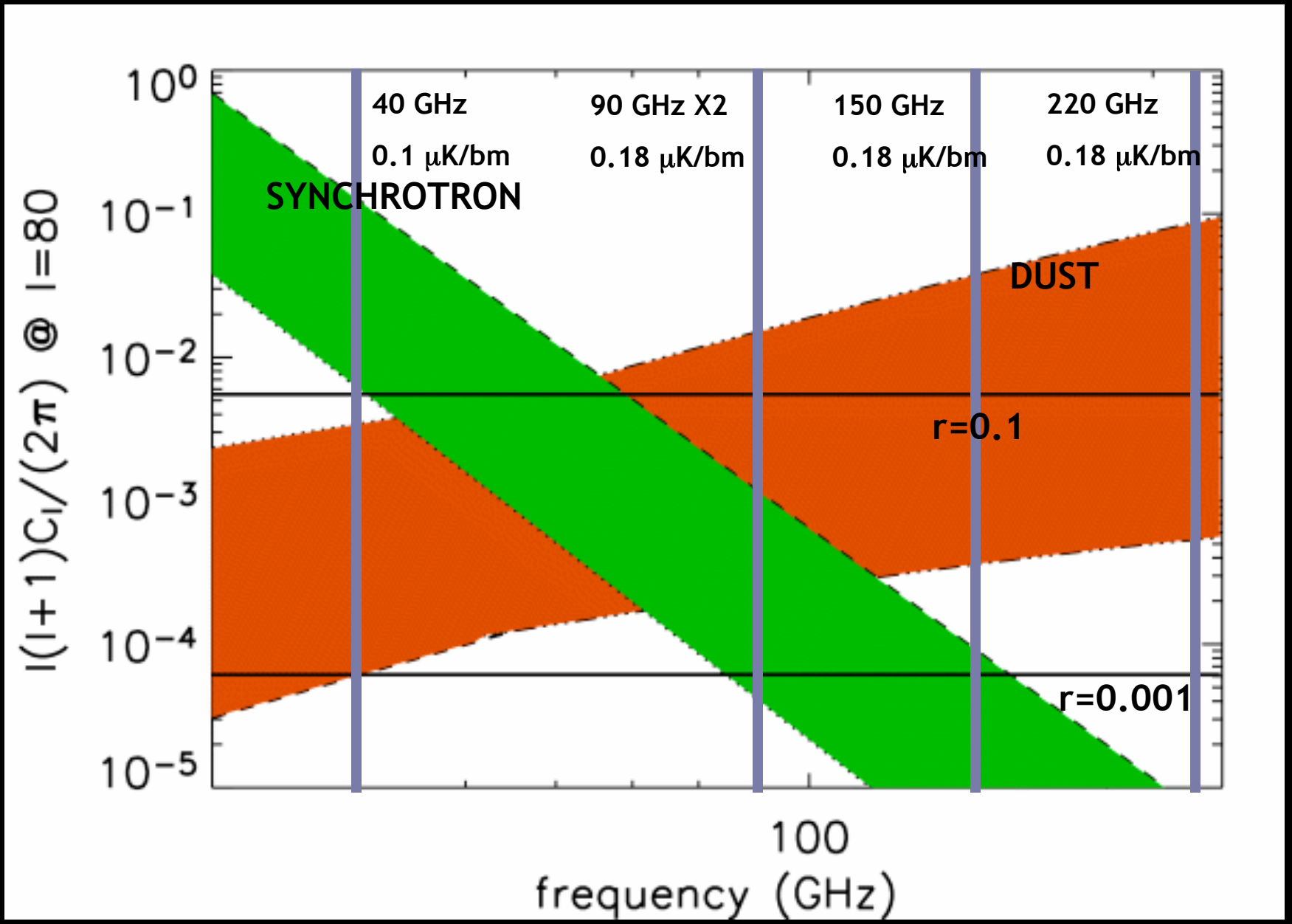

Sky coverage of experiments

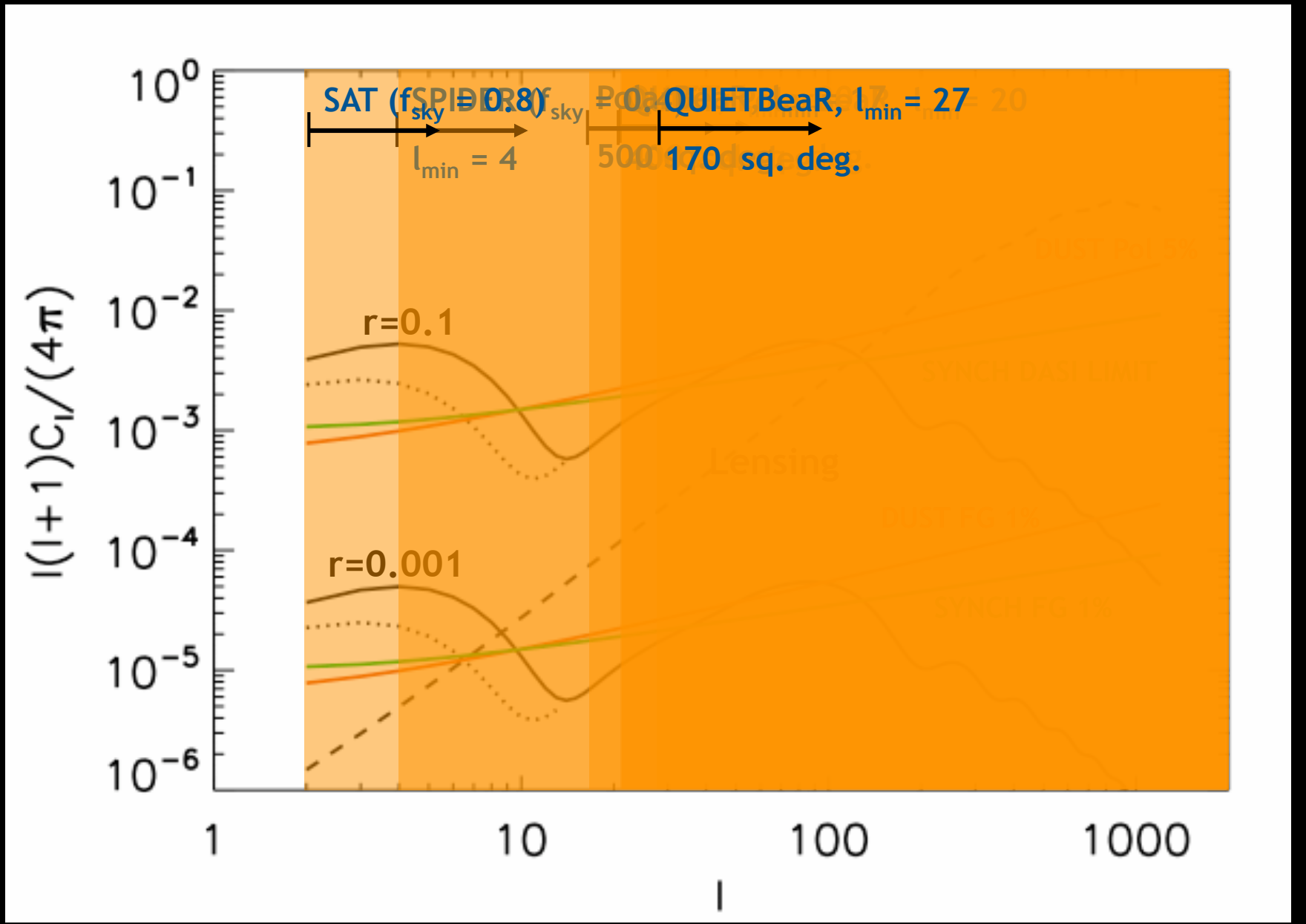

L-dependence of Noise (Space-based experiment)

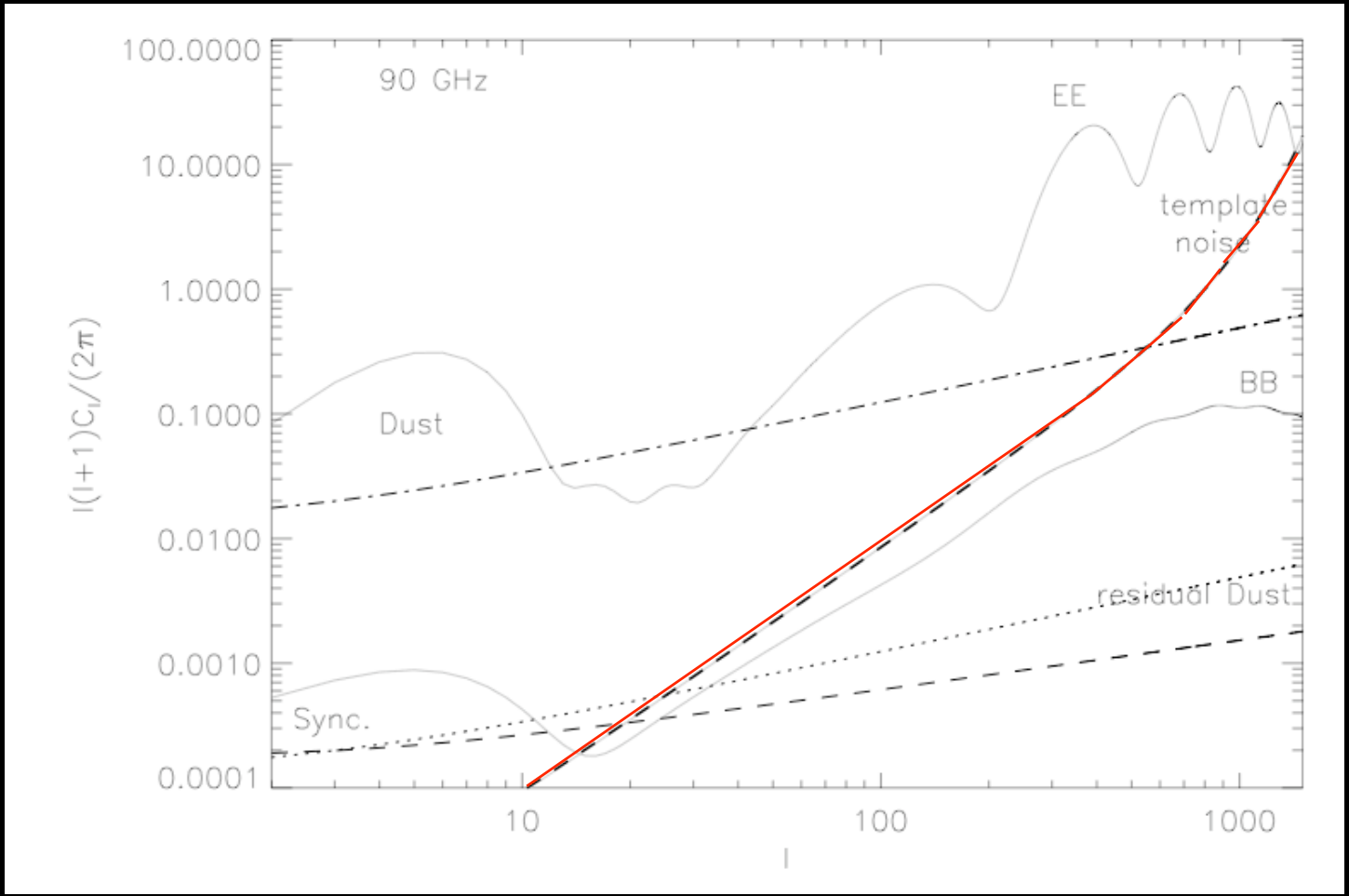

Approximate range of primordial B-modes accessible to upcoming experiments

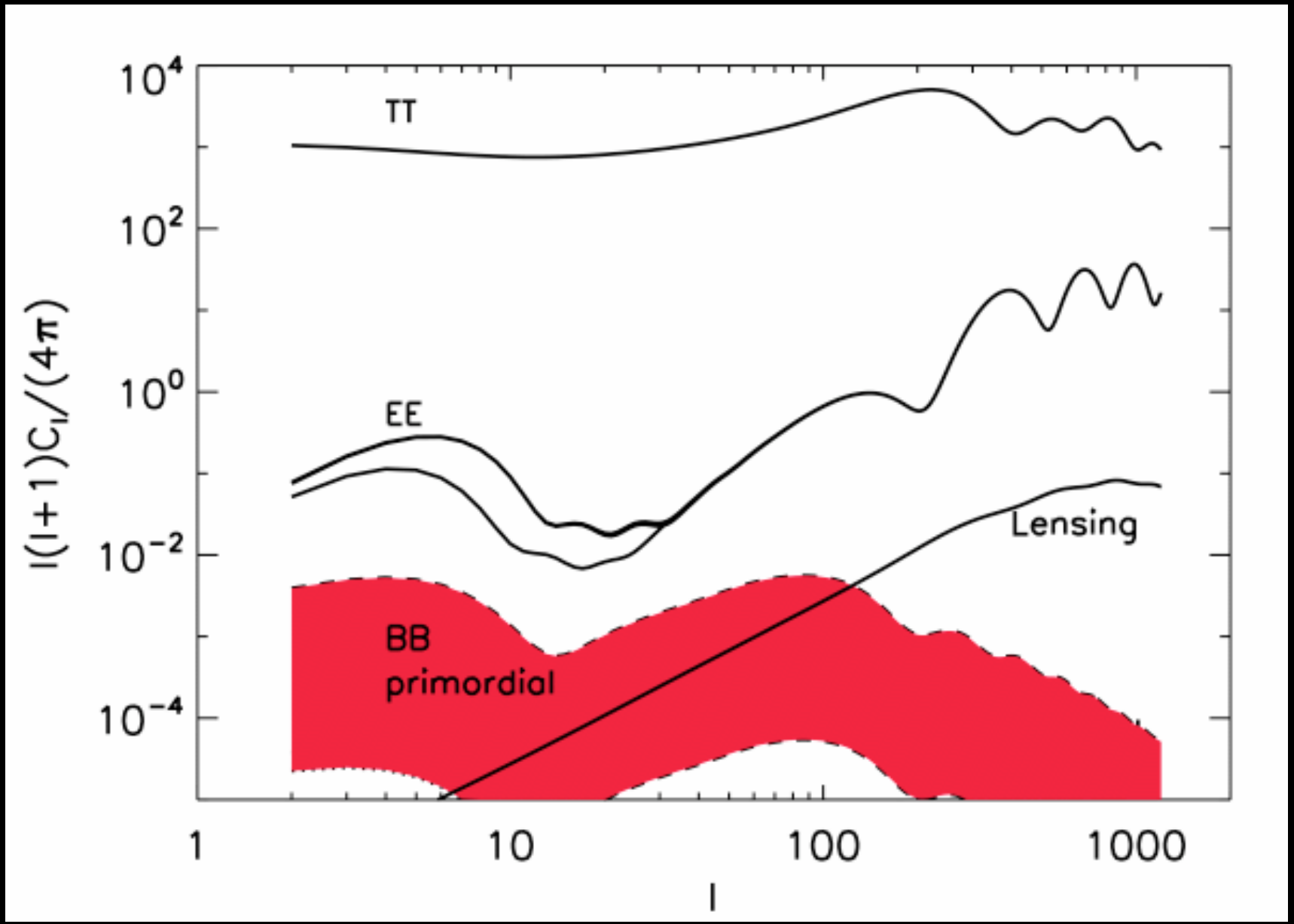

Measurement vs. detection

There are two different approaches in reporting an experiment's capability to constrain r.

1. Consider the null hypothesis of zero signal (i.e. r=0) and then ask with what significance a non-zero value of r could be distinguished from the null hypothesis:
   - Gives statistical significance of a detection but does not give a measurement of r.

2. Bayesian maximum likelihood analysis with the cosmic variance contribution for non-zero r included in the error calculation:
   - Gives a measurement of r with an error-bar. This is what is needed to constrain inflationary models.
   - Hence we do not report the minimum r that can be distinguished from zero, but error-bars for several fiducial r values.

For detailed results, see Table 6 of astro-ph/0506036

Table 6. Constraints on all parameters. IDEAL denotes an ideal experiment(no foregrounds, cosmic variance dominated). SAT denotes a space-based experiment. CR means that the consistency relation for n_T, $n_t = -r/8$ has been imposed. FLT means that flatness has been imposed, this does not affect the errors on the parameters relevant to inflation. FG denotes that galactic foregrounds has been considered. FG1% means that their residual contamination is reduced to 1% while FG10% means that foreground contamination has been reduced to 10%. The experimental specifications used for obtaining these constraints are reported in Table 7. The error on the amplitude does not include possible calibration errors which are likely to dominate. These forecasts have been computed for a fiducial value of $\tau = 0.164$ except where explicitly specified. As the BB signal on large scales is boosted by τ roughly as τ^2, lower values of τ will degrade the significance of these forecasts. For fiducial τ one sigma below the best fit value the detectability of $r = 0.01$ ($r = 0.03$) from $\ell < 20$ is equivalent to the detectability of $r = 0.03$ ($r = 0.1$) in the best fit model. This consideration affects only large sky coverage experiments which probe the "reionization bump" in the BB spectrum at $\ell < 10$ and does not affect the smaller scale ground-based experiments.

r	case	Δr	Δn	Δn_t	$\Delta dn/d\ln k$	ΔZ	$\Delta\omega_b$	$\Delta\omega_c$	Δh	$\Delta\Omega_K$	Δ_A
0.01		0.001	0.0017	0.056	0.0034	0.0033	6×10^{-5}	0.00027	0.003	0.0006	0.004
0.03	IDEAL	0.0028	0.0017	0.047	0.0036	0.0034	6.4×10^{-5}	0.00026	0.0033	0.0006	0.004
0.1		0.0063	0.0018	0.035	0.0035	0.0036	6×10^{-5}	0.00020	0.0023	0.0006	0.004
0.01		0.00045	0.0017	–	0.0036	0.0032	6.1×10^{-5}	0.00025	0.003	0.0006	0.0038
0.03	IDEAL,	0.00074	0.0017	–	0.0036	0.0032	6.4×10^{-5}	0.00026	0.0032	0.00060	0.0038
0.1	CR	0.0015	0.0017	–	0.0036	0.0032	6.4×10^{-5}	0.00026	0.0024	0.0006	0.0038
0.01	IDEAL	0.000021	0.0021	0.0019	0.0038	0.0038	6.5×10^{-5}	0.00072	0.0057	0.0006	0.0048
0.03	DL	0.000063	0.0021	0.0019	0.0038	0.0038	6.5×10^{-5}	0.00072	0.0057	0.0006	0.0049
0.01	IDEAL	0.000016	0.0021	–	0.0038	0.0038	6.5×10^{-5}	0.00072	0.0057	0.0006	0.0048
0.03	DL CR	0.000049	0.0021	–	0.0038	0.0038	6.4×10^{-5}	0.00072	0.0057	0.0006	0.0049
0.01		0.0030	0.0023	0.098	0.0046	0.0053	8.4×10^{-5}	0.00053	0.0055	0.00078	0.0066
0.03	SAT	0.0048	0.0023	0.069	0.0046	0.0053	8.4×10^{-5}	0.00054	0.0056	0.00080	0.0066
0.1		0.010	0.0023	0.056	0.0046	0.0055	8.4×10^{-5}	0.00055	0.0058	0.00082	0.0068
0.01	SAT	0.0030	0.0023	0.096	0.0046	0.0049	8.3×10^{-5}	0.00050	0.0023	–	0.0062
0.03		0.0047	0.0023	0.068	0.0046	0.0050	8.3×10^{-5}	0.00051	0.0023	–	0.0062
0.1	FLT	0.010	0.0023	0.054	0.0046	0.0050	8.3×10^{-5}	0.00052	0.0023	–	0.0062
0.01		0.0011	0.0023	–	0.0046	0.0052	8.3×10^{-5}	0.00051	0.0054	0.00078	0.0065
0.03	SAT	0.0017	0.0023	–	0.0046	0.0050	8.3×10^{-5}	0.00051	0.0054	0.00078	0.0063
0.1	CR	0.0028	0.0023	–	0.0046	0.0049	8.2×10^{-5}	0.00051	0.0054	0.00080	0.0062
0.01	SAT FG1% FLT	0.0031	0.0023	0.098	0.0046	0.0049	8.3×10^{-5}	0.0005	0.0024	–	0.0063
0.01	+CR	0.001	0.0022	–	0.0046	0.0049	8.3×10^{-5}	0.0005	0.0023	–	0.0062
0.01	SAT, DASI50%, $\tau = 0.1$ FG1% FLT	0.0030	0.0021	0.1	0.0044	0.0040	7.6×10^{-5}	0.00047	0.0021	–	0.0045
0.01	+CR	0.0012	0.0020	–	0.0043	0.040	7.6×10^{-5}	0.00046	0.0020	–	0.0045
0.0001	SAT FLT	0.00019	0.0023	0.43	0.0046	0.005	8.3×10^{-5}	0.00051	0.0023	–	0.0063
0.001	FG1% DASI50%	0.0013	0.0023	0.31	0.0046	0.005	8.3×10^{-5}	0.0005	0.0023	–	0.0063
0.0001	SAT FLT CR	0.00012	0.0023	–	0.0046	0.005	8.3×10^{-5}	0.0005	0.0023	–	0.0063
0.001	FG1% DASI50%	0.0003	0.0023	–	0.0046	0.005	8.3×10^{-5}	0.0005	0.0023	–	0.0063
0.01	SAT FG10% FLT	0.0035	0.0023	0.11	0.0046	0.005	8.3×10^{-5}	0.00052	0.0024	–	0.0063
0.01	+CR	0.0013	0.0023	–	0.0046	0.0049	8.3×10^{-5}	0.0005	0.0023	–	0.0063
0.001	SAT FLT FG 10% DASI50%	0.00051	0.0023	0.13	0.0046	0.0050	8.3×10^{-5}	0.00051	0.0023	–	0.0063
0.001	SAT FLT CR FG 10% DASI50%	0.00042	0.0023	–	0.0046	0.0050	8.3×10^{-5}	0.00051	0.0023	–	0.0063
0.0001	SAT NO NOISE FG1% FLT DASI 50%	0.00007	0.0019	0.17	0.0037	0.005	7.4×10^{-5}	0.0022	0.0008	–	0.005
0.0001	+CR	0.000057	0.0019	–	0.0037	0.005	7.4×10^{-5}	0.0022	0.0008	–	0.005

B-modes and Inflation

Measurement of the amplitude of tensor modes fixes Hubble parameter H during inflation when relevant scales are leaving horizon; alternatively, fixes scalar field potential and first derivative. e.g. Liddle & Lyth (1993), Copeland et al. (1993), Liddle (1994)

$$H \equiv \dot{a}/a \approx \frac{1}{M_{Pl}}\sqrt{\frac{V}{3}}$$

$$r = \frac{2V}{3\pi^2 M_{Pl}{}^4 \Delta_R{}^2(k_0)} = 8 M_{Pl}{}^2 \left(\frac{V'}{V}\right)^2$$

$$V^{1/4} \leq 3.3 \times 10^{16}\, r^{1/4}\ \mathrm{GeV}$$

Current compilation of CMB+LSS cosmological data Seljak et al. (2004) gives a 95% upper limit:

$$r < 0.36$$

$$V^{1/4} \leq 2.6 \times 10^{16}\,\mathrm{GeV}$$

$$V^{1/4} \leq 1.1 \times 10^{-2}\, M_{Pl}$$

B-modes and Inflation (contd)

Can take point of view that **inflaton is a fundamental field**, and use effective field theory techniques to describe it. Effective potential can be expanded in non-renormalizable operators suppressed by e.g. Planck mass: e.g. Liddle & Lyth (1993), Copeland et al. (1993), Liddle (1994)

$$V(\phi) = V_0 + \frac{1}{2}m^2\phi^2 + \phi^4 \sum_{p=0}^{\infty} \lambda_p \left(\frac{\phi}{m_{Pl}}\right)^p$$

For series expansion to be convergent and EFT to be self-consistent, require $\phi << m_{Pl.}$ Lyth (1997) showed that the width of the potential $\Delta\phi$ can also be related to r:

$$\frac{\Delta\phi}{m_{Pl}} \approx 0.5 \left(\frac{r}{0.07}\right)^{1/2}$$

High values of r require changes in $\Delta\phi$ of order $m_{Pl.}$

Result used to argue that that very small tensor modes are expected in a realistic inflationary universe.

Implications of detection of primordial GW background

Alternative approach: Monte Carlo simulation of the inflationary flow equations.
(a la Kinney 2002, Easther & Kinney 2002)

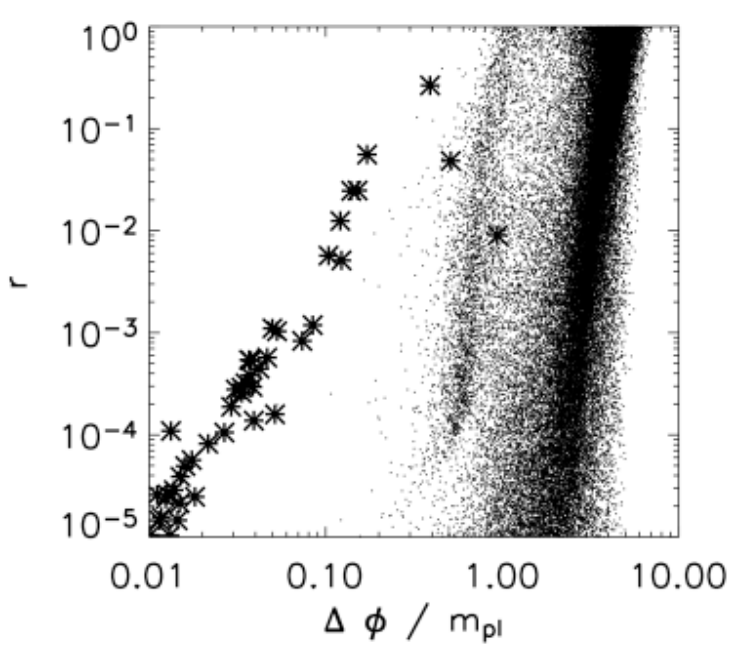

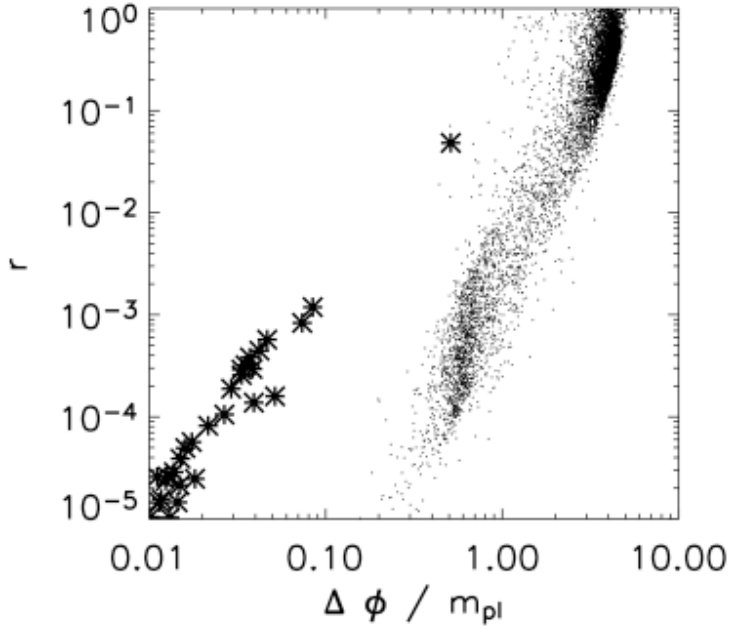

Apply constraints from CMB+LSS (Seljak et al. 2004)

r is still a very steep function of $\Delta\phi$ (Efstathiou & Mack 2005):

$$\frac{\Delta\phi}{m_{Pl}} \approx 6\, r^{1/4}$$

Hubble slow roll & Hamilton Jacobi Formulation

$$\begin{aligned} \dot{\phi} &= -2M_{\rm pl}^2 H'(\phi), \\ [H'(\phi)]^2 - \frac{3}{2M_{\rm pl}^2} H^2(\phi) &= -\frac{1}{2M_{\rm pl}^4} V(\phi). \end{aligned}$$

$$\epsilon_H \equiv 2M_{\rm pl}^2 \left(\frac{H'(\phi)}{H(\phi)} \right)^2$$

$$^{\ell}\lambda_H \equiv \left(\frac{m_{\rm Pl}}{4\pi} \right)^{\ell} \frac{(H')^{\ell-1}}{H^{\ell}} \frac{d^{(\ell+1)}H}{d\phi^{(\ell+1)}}.$$

Monte-Carlo generate with some priors, equivalent to generate potentials

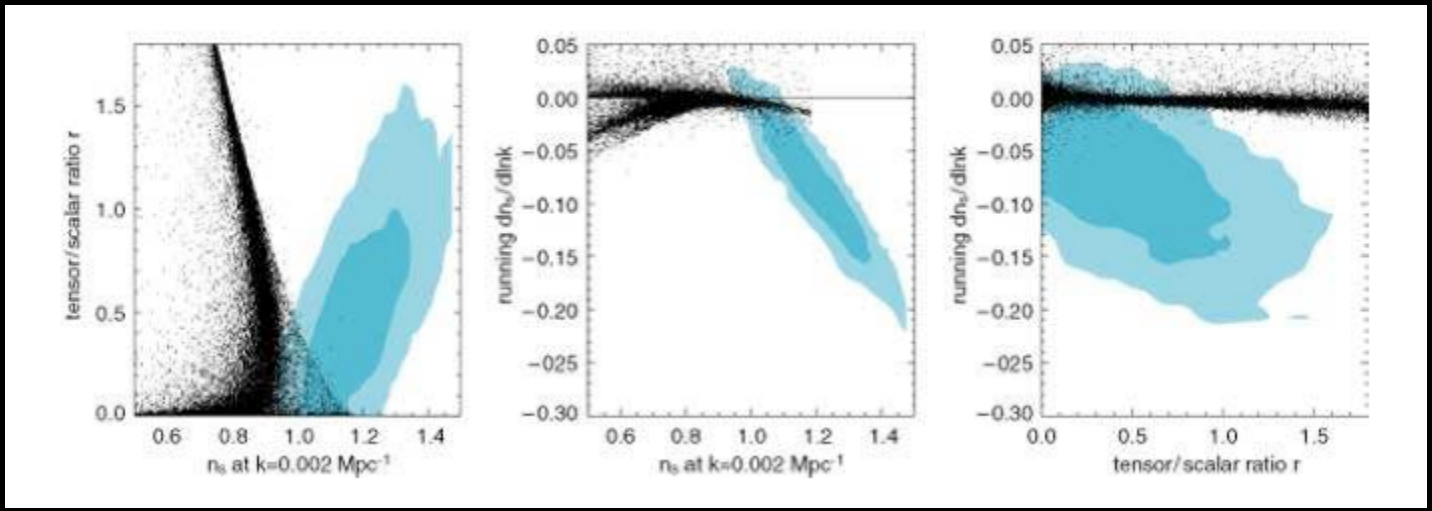

Peiris et al. 2003

Implications of detection of primordial GW background

Alternative approach: Monte Carlo simulation of the inflationary flow equations.
(a la Kinney 2002, Easther & Kinney 2002)

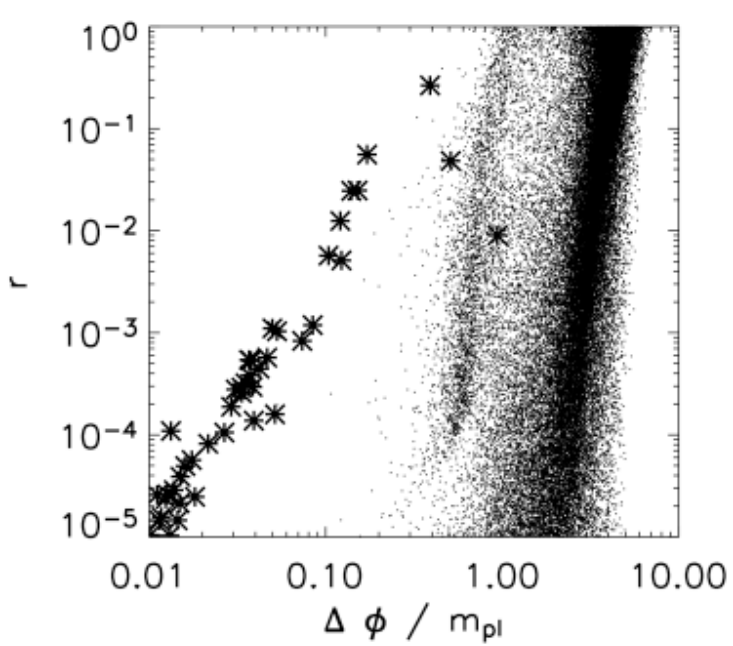

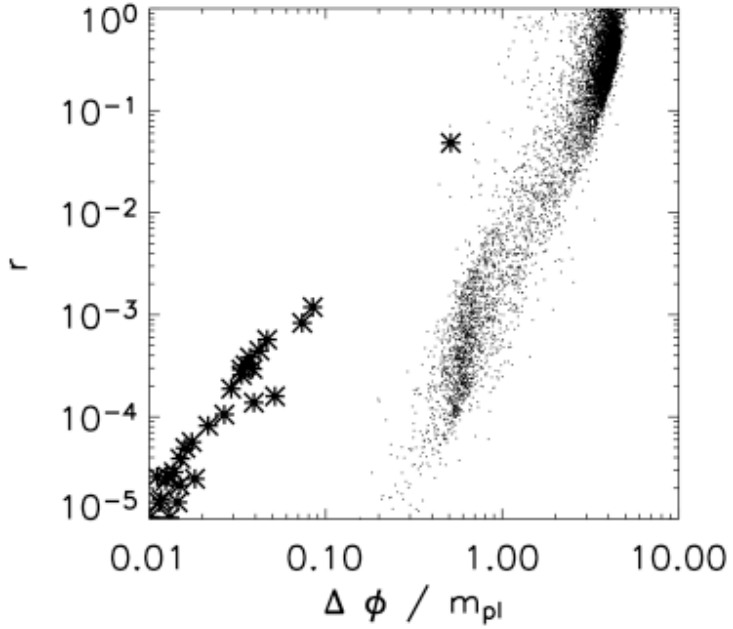

Apply constraints from CMB+LSS (Seljak et al. 2004)

r is still a very steep function of $\Delta\phi$ (Efstathiou & Mack 2005):

$$\frac{\Delta\phi}{m_{Pl}} \approx 6\, r^{1/4}$$

For detailed results, see Table 6 of Verde, Peiris, RJ JCAP (2006)

Table 6. Constraints on all parameters. IDEAL denotes an ideal experiment(no foregrounds, cosmic variance dominated). SAT denotes a space-based experiment. CR means that the consistency relation for n_T, $n_t = -r/8$ has been imposed. FLT means that flatness has been imposed, this does not affect the errors on the parameters relevant to inflation. FG denotes that galactic foregrounds has been considered. FG1% means that their residual contamination is reduced to 1% while FG10% means that foreground contamination has been reduced to 10%. The experimental specifications used for obtaining these constraints are reported in Table 7. The error on the amplitude does not include possible calibration errors which are likely to dominate. These forecasts have been computed for a fiducial value of $\tau = 0.164$ except where explicitly specified. As the BB signal on large scales is boosted by τ roughly as τ^2, lower values of τ will degrade the significance of these forecasts. For fiducial τ one sigma below the best fit value the detectability of $r = 0.01$ ($r = 0.03$) from $\ell < 20$ is equivalent to the detectability of $r = 0.03$ ($r = 0.1$) in the best fit model. This consideration affects only large sky coverage experiments which probe the "reionization bump" in the BB spectrum at $\ell < 10$ and does not affect the smaller scale ground-based experiments.

r	case	Δr	Δn	Δn_t	$\Delta dn/d\ln k$	ΔZ	$\Delta\omega_b$	$\Delta\omega_c$	Δh	$\Delta\Omega_K$	Δ_A
0.01		0.001	0.0017	0.056	0.0034	0.0033	6×10^{-5}	0.00027	0.003	0.0006	0.004
0.03	IDEAL	0.0028	0.0017	0.047	0.0036	0.0034	6.4×10^{-5}	0.00026	0.0033	0.0006	0.004
0.1		0.0063	0.0018	0.035	0.0035	0.0036	6×10^{-5}	0.00020	0.0023	0.0006	0.004
0.01		0.00045	0.0017	–	0.0036	0.0032	6.1×10^{-5}	0.00025	0.003	0.0006	0.0038
0.03	IDEAL,	0.00074	0.0017	–	0.0036	0.0032	6.4×10^{-5}	0.00026	0.0032	0.00060	0.0038
0.1	CR	0.0015	0.0017	–	0.0036	0.0032	6.4×10^{-5}	0.00026	0.0024	0.0006	0.0038
0.01	IDEAL	0.000021	0.0021	0.0019	0.0038	0.0038	6.5×10^{-5}	0.00072	0.0057	0.0006	0.0048
0.03	DL	0.000063	0.0021	0.0019	0.0038	0.0038	6.5×10^{-5}	0.00072	0.0057	0.0006	0.0049
0.01	IDEAL	0.000016	0.0021	–	0.0038	0.0038	6.5×10^{-5}	0.00072	0.0057	0.0006	0.0048
0.03	DL CR	0.000049	0.0021	–	0.0038	0.0038	6.4×10^{-5}	0.00072	0.0057	0.0006	0.0049
0.01		0.0030	0.0023	0.098	0.0046	0.0053	8.4×10^{-5}	0.00053	0.0055	0.00078	0.0066
0.03	SAT	0.0048	0.0023	0.069	0.0046	0.0053	8.4×10^{-5}	0.00054	0.0056	0.00080	0.0066
0.1		0.010	0.0023	0.056	0.0046	0.0055	8.4×10^{-5}	0.00055	0.0058	0.00082	0.0068
0.01	SAT	0.0030	0.0023	0.096	0.0046	0.0049	8.3×10^{-5}	0.00050	0.0023	–	0.0062
0.03		0.0047	0.0023	0.068	0.0046	0.0050	8.3×10^{-5}	0.00051	0.0023	–	0.0062
0.1	FLT	0.010	0.0023	0.054	0.0046	0.0050	8.3×10^{-5}	0.00052	0.0023	–	0.0062
0.01		0.0011	0.0023	–	0.0046	0.0052	8.3×10^{-5}	0.00051	0.0054	0.00078	0.0065
0.03	SAT	0.0017	0.0023	–	0.0046	0.0050	8.3×10^{-5}	0.00051	0.0054	0.00078	0.0063
0.1	CR	0.0028	0.0023	–	0.0046	0.0049	8.2×10^{-5}	0.00051	0.0054	0.00080	0.0062
0.01	SAT FG1% FLT	0.0031	0.0023	0.098	0.0046	0.0049	8.3×10^{-5}	0.0005	0.0024	–	0.0063
0.01	+CR	0.001	0.0022	–	0.0046	0.0049	8.3×10^{-5}	0.0005	0.0023	–	0.0062
0.01	SAT, DASI50%, $\tau = 0.1$ FG1% FLT	0.0030	0.0021	0.1	0.0044	0.0040	7.6×10^{-5}	0.00047	0.0021	–	0.0045
0.01	+CR	0.0012	0.0020	–	0.0043	0.040	7.6×10^{-5}	0.00046	0.0020	–	0.0045
0.0001	SAT FLT	0.00019	0.0023	0.43	0.0046	0.005	8.3×10^{-5}	0.00051	0.0023	–	0.0063
0.001	FG1% DASI50%	0.0013	0.0023	0.31	0.0046	0.005	8.3×10^{-5}	0.0005	0.0023	–	0.0063
0.0001	SAT FLT CR	0.00012	0.0023	–	0.0046	0.005	8.3×10^{-5}	0.0005	0.0023	–	0.0063
0.001	FG1% DASI50%	0.0003	0.0023	–	0.0046	0.005	8.3×10^{-5}	0.0005	0.0023	–	0.0063
0.01	SAT FG10% FLT	0.0035	0.0023	0.11	0.0046	0.005	8.3×10^{-5}	0.00052	0.0024	–	0.0063
0.01	+CR	0.0013	0.0023	–	0.0046	0.0049	8.3×10^{-5}	0.0005	0.0023	–	0.0063
0.001	SAT FLT FG 10% DASI50%	0.00051	0.0023	0.13	0.0046	0.0050	8.3×10^{-5}	0.00051	0.0023	–	0.0063
0.001	SAT FLT CR FG 10% DASI50%	0.00042	0.0023	–	0.0046	0.0050	8.3×10^{-5}	0.00051	0.0023	–	0.0063
0.0001	SAT NO NOISE FG1% FLT DASI 50%	0.00007	0.0019	0.17	0.0037	0.005	7.4×10^{-5}	0.0022	0.0008	–	0.005
0.0001	+CR	0.000057	0.0019	–	0.0037	0.005	7.4×10^{-5}	0.0022	0.0008	–	0.005

Current constraints

r<0.36 (CMB+LSS compilation from Seljak et al. (2004))

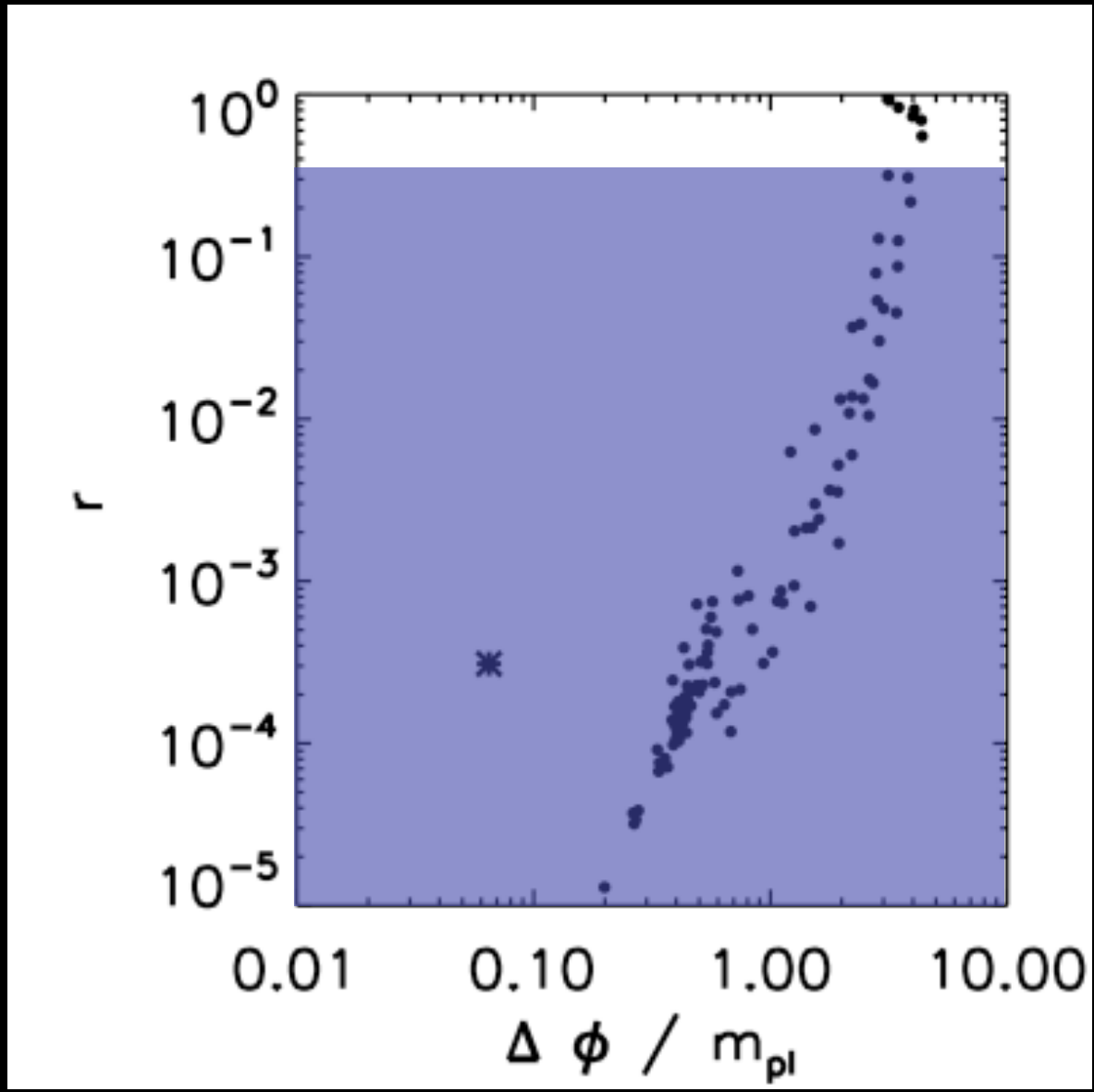

r = 0.1

QUIET FG1% and PolarBeaR FG1% can make ~3σ measurement

What's "above water" can be measured and these models can be studied

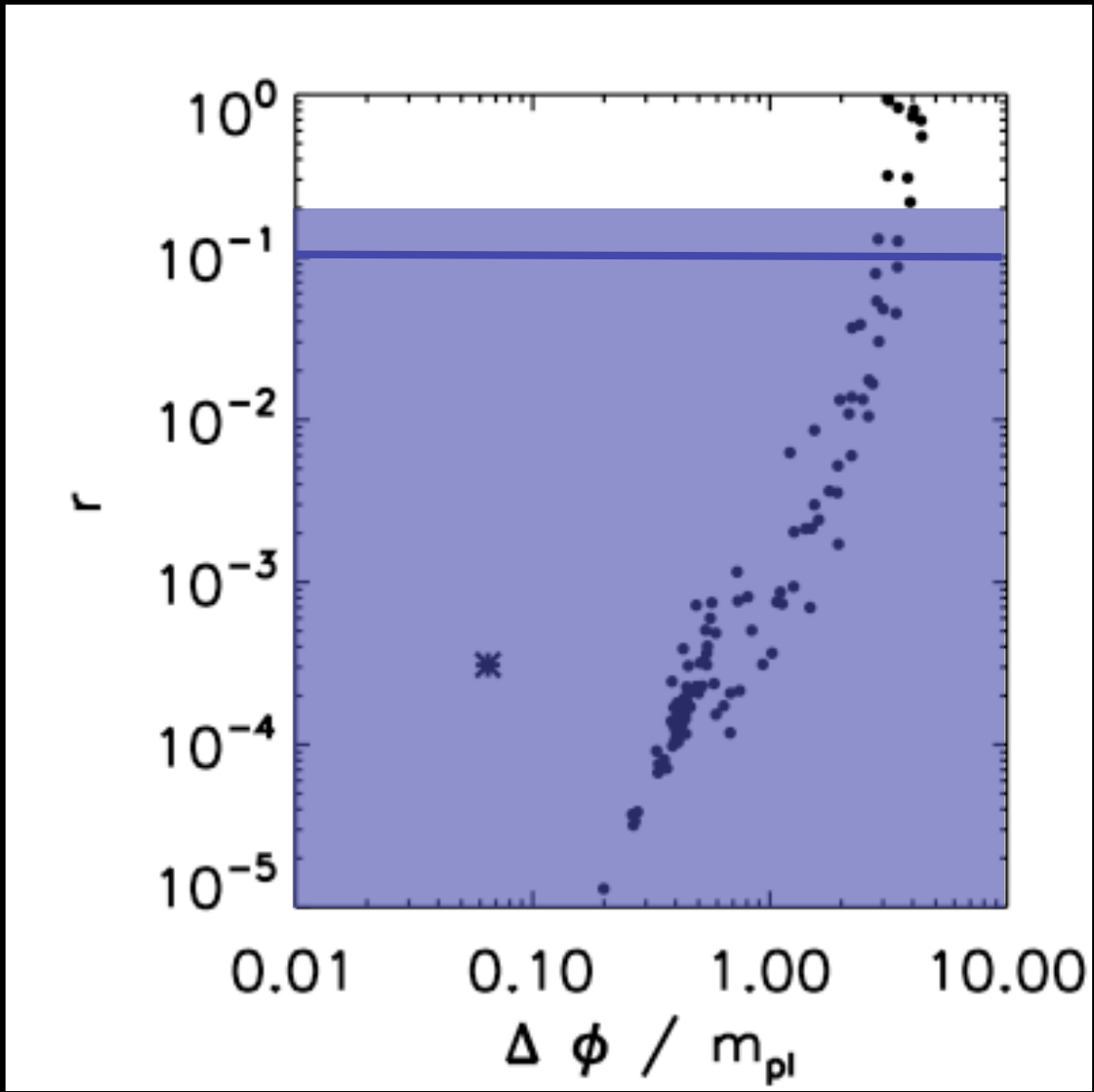

r = 0.03

QUIET + PolarBeaR FG1% can make 3σ measurement

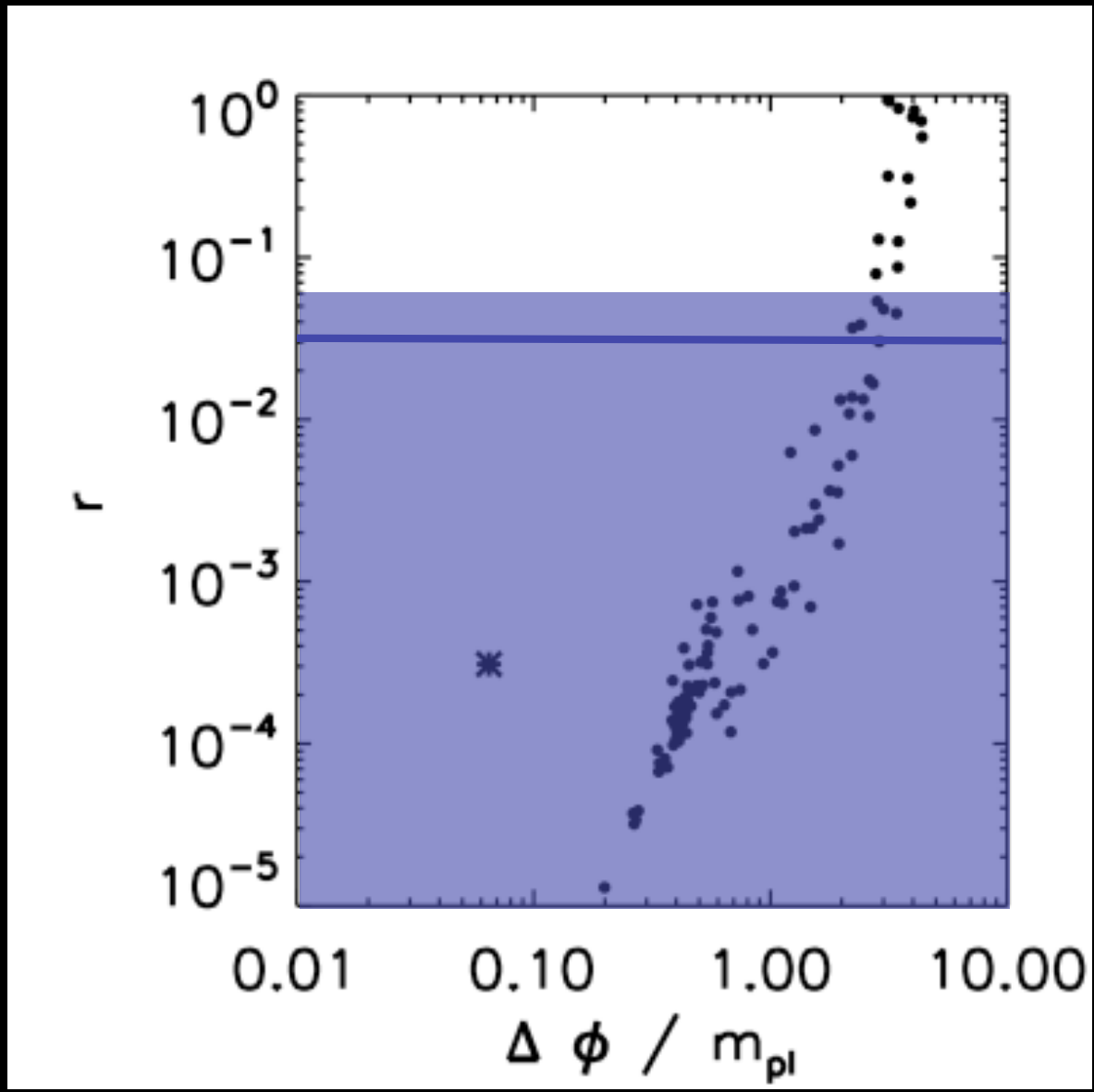

r = 0.01

QUIETBeaR FG1% (3σ), SPIDER FG1%, τ=0.1 (~3σ), SAT FG10% (~7σ)

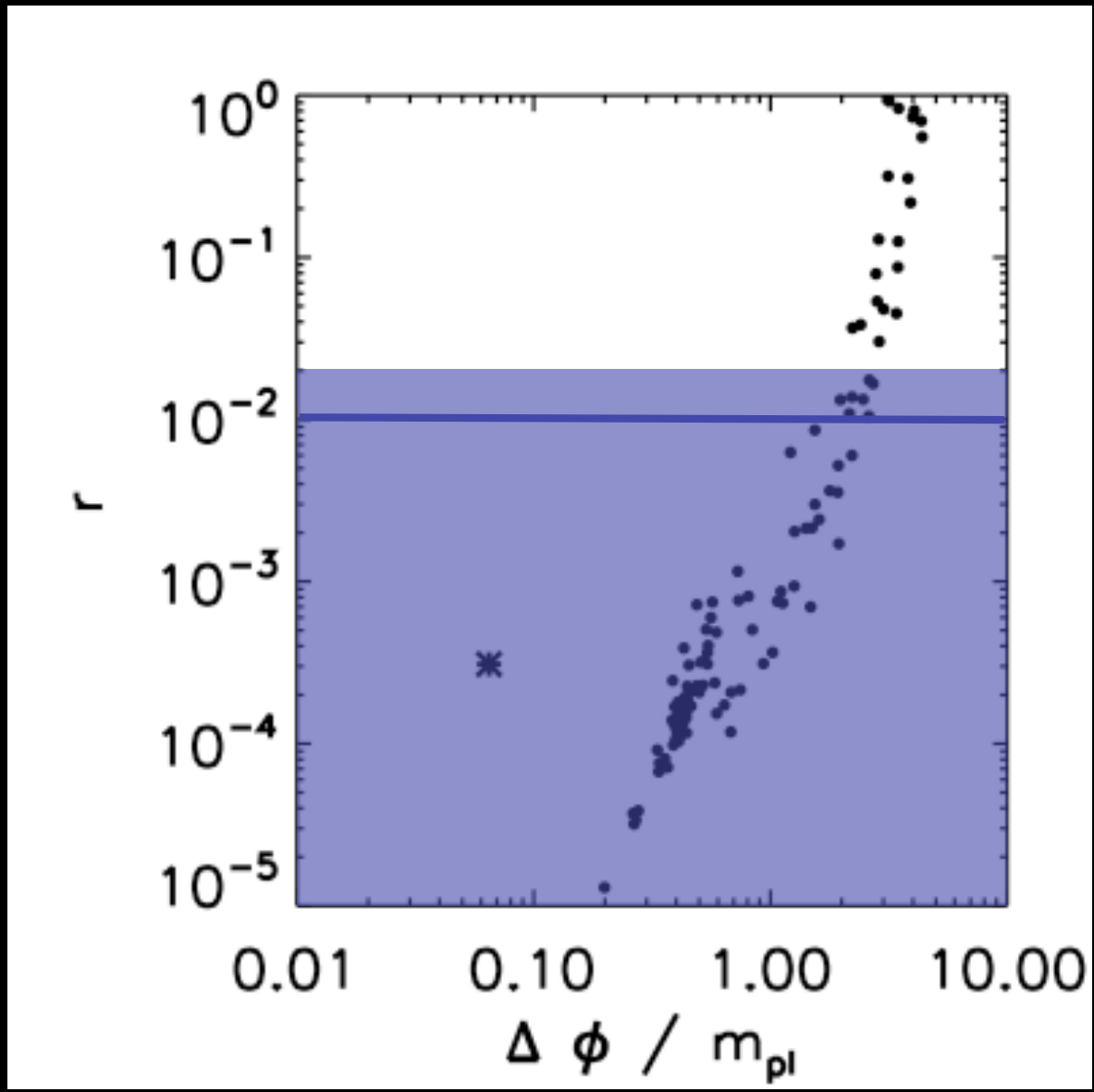

r = 0.001

SAT FG10% DASI 50% (2.4σ), SAT FG1% DASI 50% (3σ)

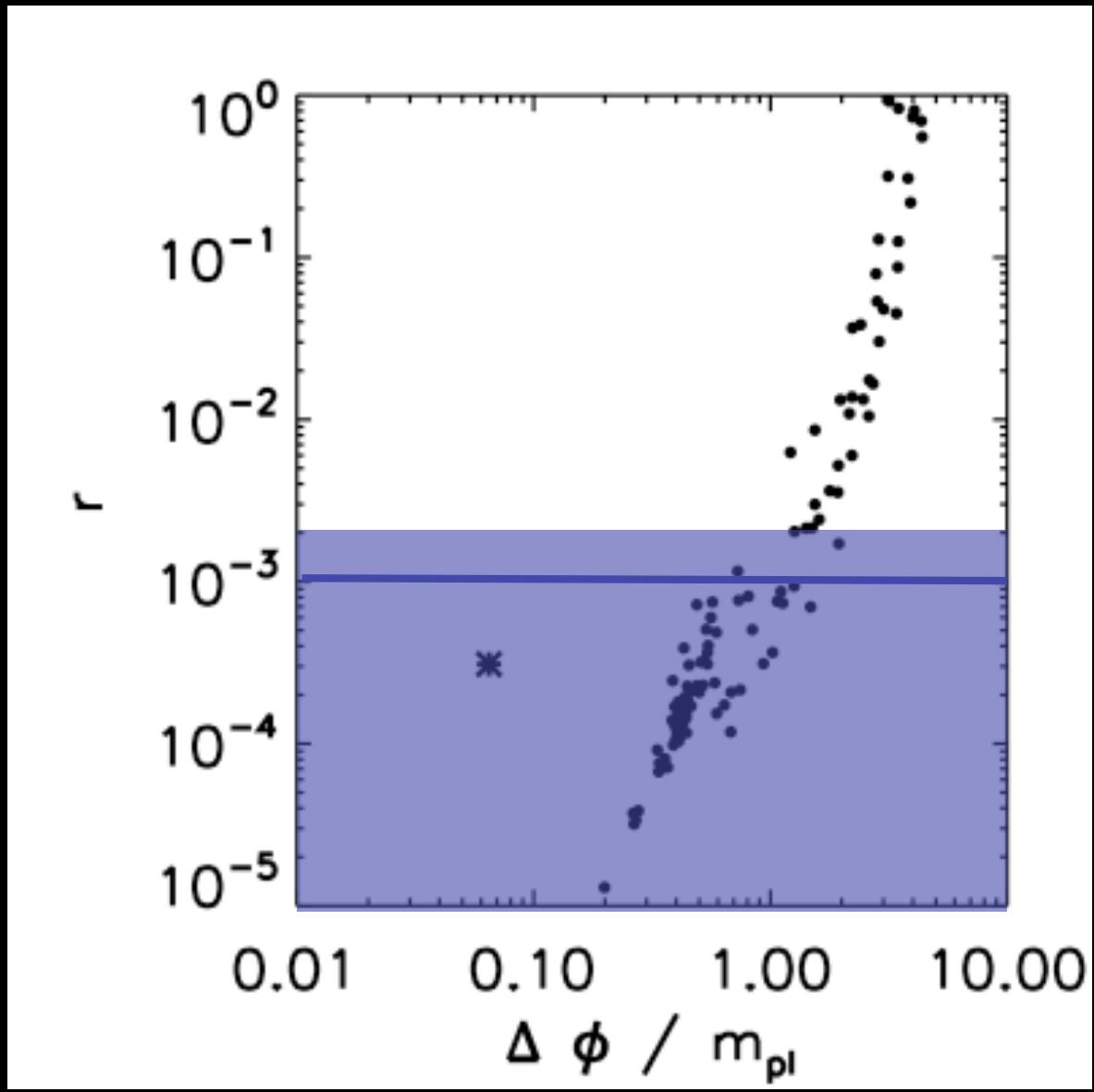

r = 0.0001

IDEAL EXPERIMENT, FG1% DASI 50% (1.8σ)

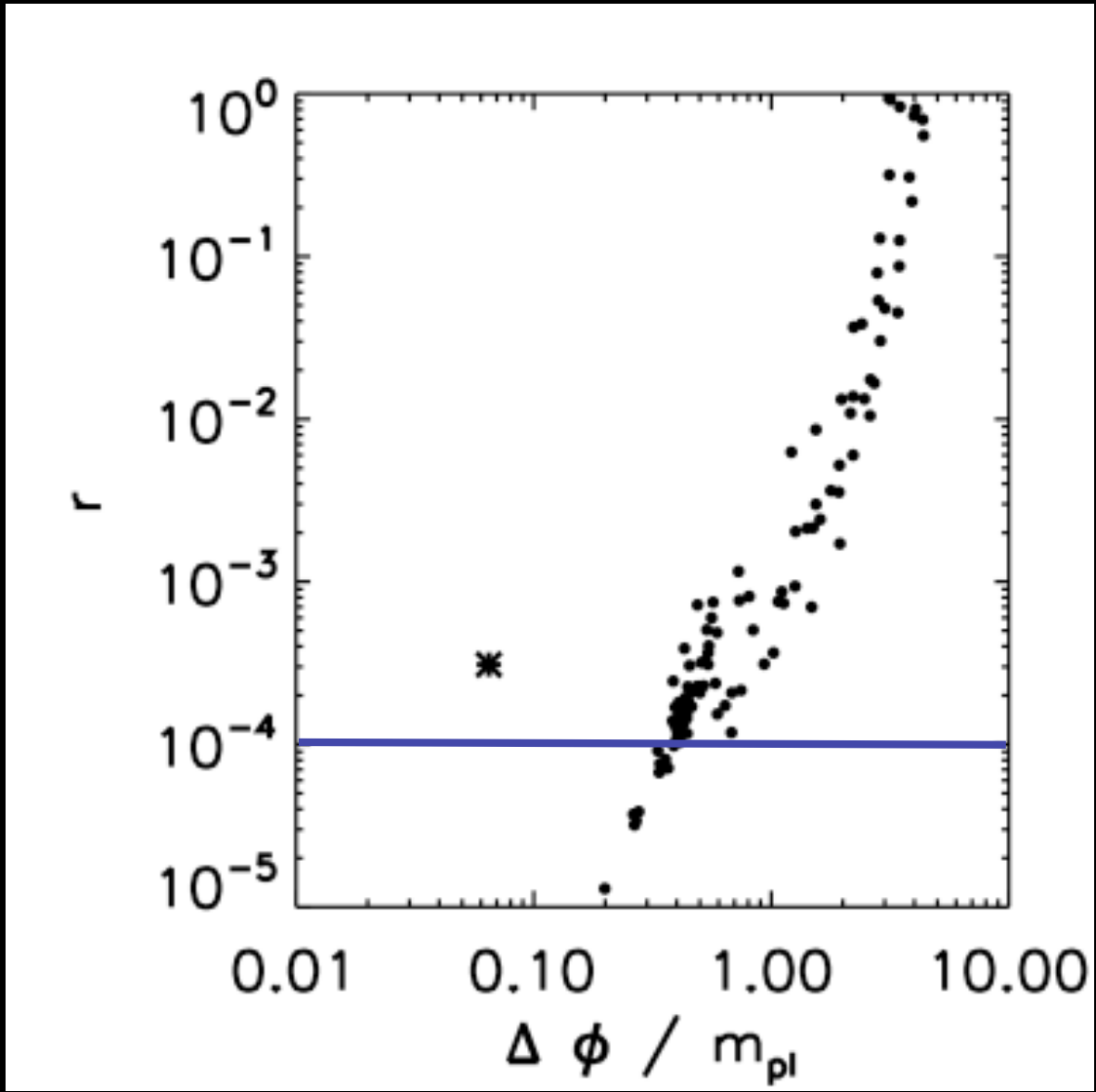

Source of r measurement

- Though full T, E, B data were used, the measurement of r comes from BB signal

- If we consider realistic satellite case but only T & E data, only upper limits can be imposed on r for $r<0.1$.

Conclusions I: Guidance for B-mode polarization experiments

- FG parameters may show spatial variations across the sky. Optimal "cosmological window" may be different for full sky and partial experiments & between different patches of the sky: one recipe may not fit all.

- **Markedly improved knowledge of amplitude and spectral/spatial dependence of foregrounds is needed to allow FG subtraction at percent level.**

- **Ground-based (partial-sky) experiments:**

  - FG contamination and noise in FG templates are the limiting factor in constraining r and the delensing implementation. Thus delensing may be used to improve r-limits in partial-sky experiments (but beware of foregrounds!).

  - Ground-based experiments can easily achieve lower noise than space-based ones and can target particularly clean areas of sky, but accurate FG templates are still needed

Conclusions I: Guidance for B-mode polarization experiments (contd.)

- **Space-based:**
  - Can easily detect r=0.001 if FG can be subtracted at the 1% level, but the main obstacle to detecting a small value of r<0.001 will come from FG contamination.
  - Can be optimized to access the low-l "reionization bump" - constraints dependent on the value of the optical depth to reionization.
- **Balloon-borne:**
  - Has access to reionization bump, cheaper than going to space, more adaptable/expandable than a space-mission.
  - Future advances to ballooning technology: e.g. "stratellite" airship combining the advantages of space-based and balloon-borne experiments may be particularly attractive.

Combination of approaches?

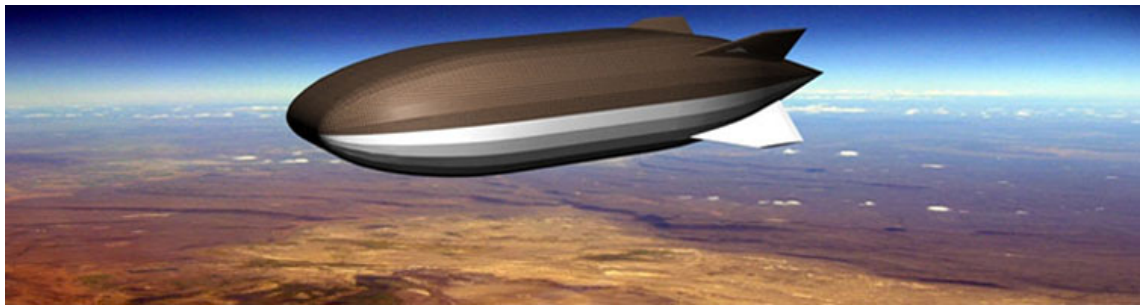

Image from http://www.sanswire.com

Conclusions II: Implications for Inflation

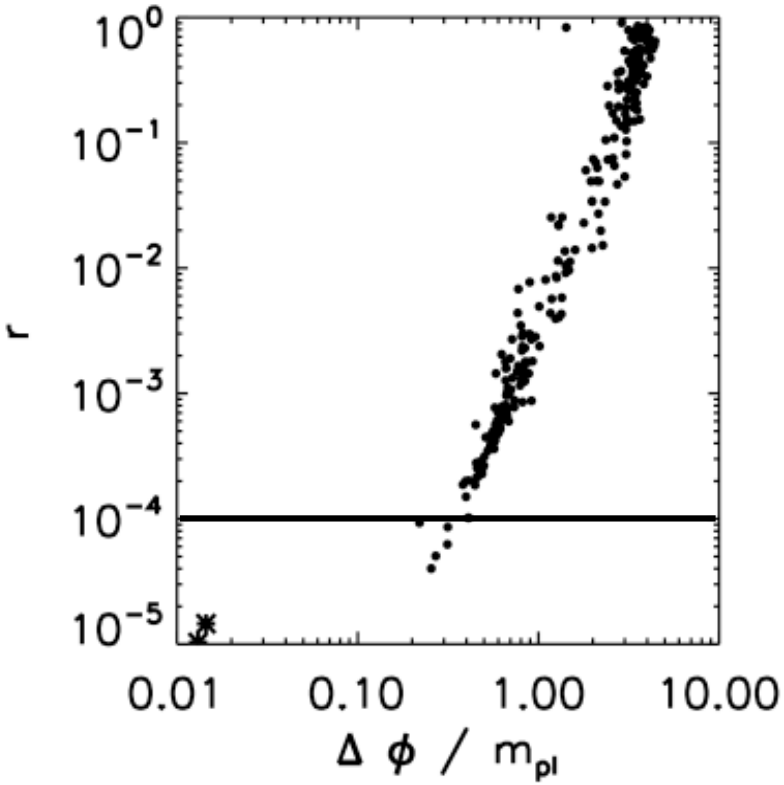

Unless we can detect $r < 10^{-4}$, **we can only test models with large field variations.**

Examples of models falling within the "detectability" regime are:

- Chaotic inflation models realized in supergravity theory where the potential has a shift symmetry Linde (2005) and references within
- Extranatural/pseudonatural inflation, in which the inflaton is an extra component of a gauge field in a 5D theory compactified in a circle Hill & Leibovich (2002), Arkani-Hamed et al. (2003)
- Purely 4d theories need more sophisticated structures in order to protect the flatness of the potential from excessive radiative corrections; in general do not predict significant tensor modes Kim et al. (2005), Arkani-Hamed et al. (2003)

Important to investigate the possibility of constructing particle-physics motivated inflationary models with $(\Delta\phi/m_{Pl}) \geq 1$ since these are likely to be the only models that can be probed by realistic CMB experiments in the near future.

Acknowledgements

- QUIET collaboration (http://cfcp.uchicago.edu/~peterh/quiet3.html)
- PolarBeaR collaboration (http://bolo.berkeley.edu/polarbear/index.html)
- SPIDER collaboration (http://www.astro.caltech.edu/~lgg/spider_front.html)
- Thanks: M. Devlin, G. Efstathiou, E. Komatsu, C.-L. Kuo, A. Lee, S. Meyer, L. Page, J. Ruhl, D. Samtleben, K. Smith, D. Spergel, H. Tran, B. Wandelt, B. Winstein

Summary

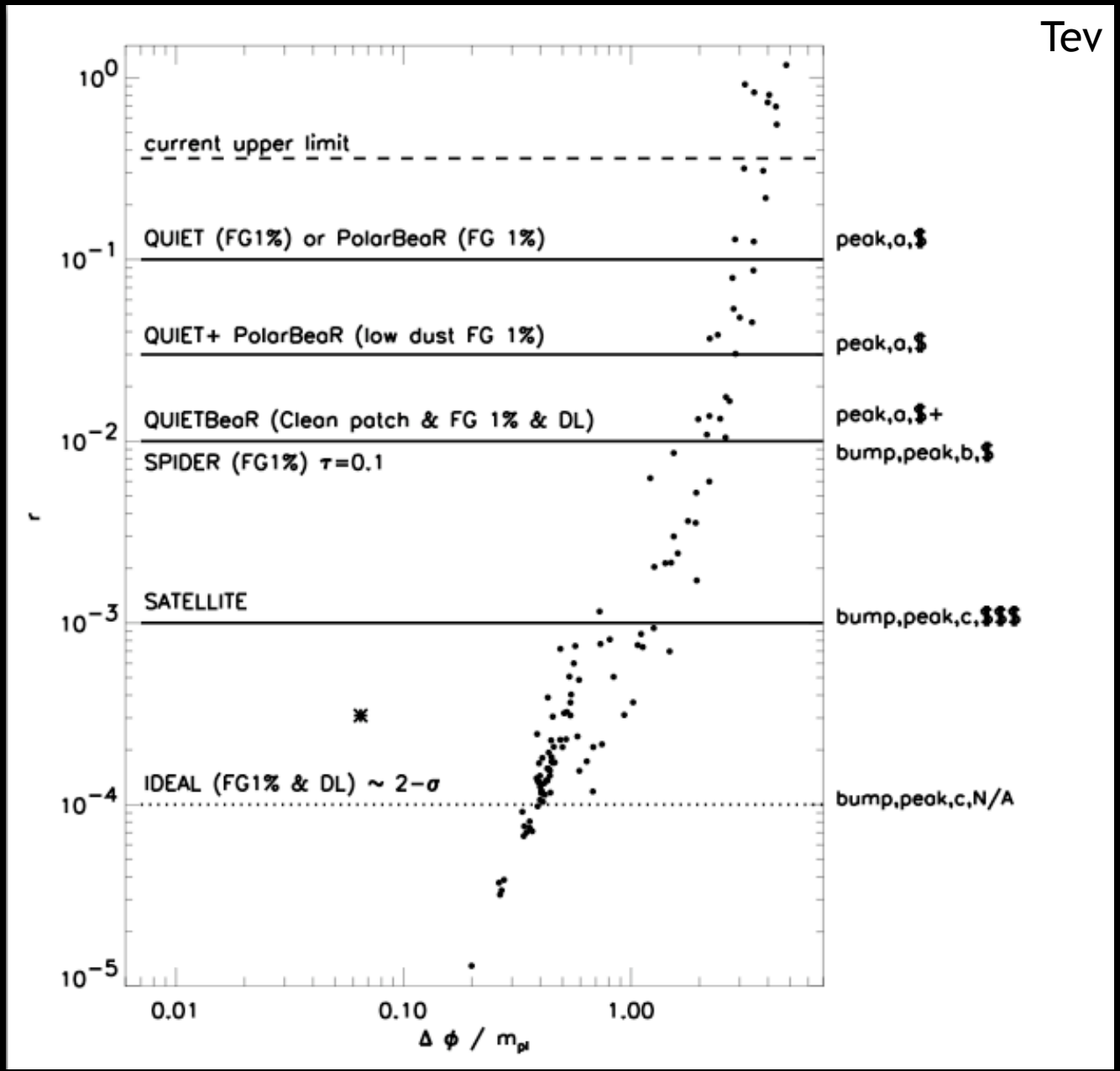
Tev
current upper limit
QUIET (FG1%) or PolarBeaR (FG 1%)
QUIET+ PolarBeaR (low dust FG 1%)
QUIETBeaR (Clean patch & FG 1% & DL)
SPIDER (FG1%) τ=0.1
SATELLITE
IDEAL (FG1% & DL) ~ 2−σ
peak,a,$
peak,a,$
peak,a,$+
bump,peak,b,$
bump,peak,c,$$$
bump,peak,c,N/A
r
Δ φ / m_pl
0.01
0.10
1.00
10^0
10^−1
10^−2
10^−3
10^−4
10^−5
3.2x10^13
1.7x10^13
9.7x10^12
5.5x10^12
3x10^12